

**N86 - 28431**

**ELECTRODYNAMICS PANEL PRESENTATION**

**James McCoy  
NASA/JSC**

Electrodynamic Panel Presentation - James E. McCoy  
NASA-JSC  
October 16, 1985

PLASMA MOTOR GENERATOR (PMG)

I. General Description -

The first two charts are typical of several being used recently to describe applications growing out of studies the last 2-3 years at NASA, which have focused around the PMG concept employing plasma producing devices at each end of the tether to allow conduction of very high currents to/from the ionosphere.

Fig. 1 - Use of the tether system as a motor/generator for day-night power storage in a solar array based power system designed to provide 100 KW continuous power. The tether also provides the capability for orbit reboost/maintenance and a limited degree of orbital maneuvering.

Fig. 2 - An expansion on the orbit reboost and "deep discharge" capability ideas from fig. 1. A 200,000 kg spacecraft in LEO can generate 250 KWHR of electrical power at the expense of 1 km altitude loss, down to some minimum safe altitude. Conversely, 250 KWHR (plus or minus efficiency factors) of electrical power can reboost the orbit by 1 km. Therefore the trade-off between 3 months at 10KW and/or 9,000 lbs of hydrazine propellant. Note that the 3 months at 10KW could be obtained at the expense of a 90 km altitude loss, instead of 9,000 kg of hydrazine.

The next five charts describe the PMG tether systems being used to calculate the estimated performance data for use in these studies, as well as design reference for engineering or theoretical analysis. The workhorse system

is called the 200 KW PMG. It is sized to suit the space station power levels and is generally suitable for most other utility applications. Other systems have also been defined for 2KW, 20KW, megawatt, and multi-megawatt application. These are essentially identical to the "200KW Reference System" except for scaling up or down in wire mass and hollow cathode (plasma contactor) capacity.

Fig. 3 - General description of the 200 KW PMG, including primary design features and trade-offs. The basic system uses no satellite at the far end(s), only a relatively small hollow cathode assembly. Special applications might add a ballast tether anchored at the end of the PMG cable (a sea anchor, or space anchor, type of function).

Fig. 4 - Descriptive summary of the "200 KW Reference System," showing major performance parameters at top, physical description and estimated mass of each component, summary of characteristics, and a breakdown of major loss terms to estimate each and show relative effect on overall efficiency figures derived at bottom line. Performance charts can be calculated by varying individual contributions according to operating current, engineering change, mass, or performance estimates, etc.

Fig. 5 - Same as fig. 4, values are for a higher capacity system operated at a lower, more "efficient" fraction of its peak capability.

Fig. 6 - Summary of most promising applications presently being studied, with some representative performance numbers.

Fig. 7 - Compares the PMG tether system with fuel cells and solar arrays at various altitudes. The tether outperforms fuel cells any time the total power required is more than a few thousand KWHR; but for long term applications solar arrays always win in the long term - except at lower altitudes where their high drag makes them impractical,

unless tethers can be used to offset that drag.

## II. Operating Principles -

The next set of charts displays the voltage drops and current contact geometries involved in operation of an electrodynamic tether, attempting to illustrate the comparative behavior of hollow cathodes, electron guns and passive collectors for current coupling into the ionosphere. The ionospheric conductivity itself is simply assumed large ( $R \approx 1/2$  ohm) if the "plasma contractor" establishes electrical contact such that the return current is spread over a sufficiently large area.

Fig. 8 - The sketch at top shows the geometry of a 10 km tether wire operating between a spacecraft (left end) and a TSS size satellite (right end). Orbital velocity is directed into the paper and magnetic field perpendicular (up), so that induced voltage is directed toward the right (causing electron current flow in the wire from satellite toward spacecraft). Contact currents at each end will tend to be confined to "flux tubes" along the magnetic field as indicated, until cross-field diffusion can occur. This confinement might contain the currents along a flux tube until reaching the E-region where increased Cowling conductivity allows closure. Relative initial dimensions are shown, for thermal electrons, KeV electrons from a gun, or 1-10 eV ions from an argon plasma source. Other factors, such as formation of magnetodynamic waves/"Alfven Wings" may be important but are not illustrated. The entire disturbance is transient, moving across the "flux tubes" at orbital velocity. The middle figure shows the various voltage

drops thru the system, assumed operating with a low resistance wire and a resistive load ( $R_L$ ) located near the spacecraft. Voltage drops occur at each end in the contact regions (sheath, electron gun, plasma cloud), which are characterized here as resistances (at B1 and B2) although they are in general very non-linear. The drop at the positive current end (B1) is often larger than the negative current (electron collecting, B2) end. The induced voltage ( $V_{XB-L} = 2 \text{ KV}$ , here) less the contact drops at both ends is the available working voltage to drive the total load  $R_L'$ . The wire resistance  $R_W$  is effectively in series with  $R_L$  as part of the total load ( $R_L' = R_L + R_W (+R_I)$ ), which also includes any significant ionospheric impedance  $R_I$ , therefore reducing the effective working voltage at the load by  $I(R_W + R_I)$ . For motor operation, these terms all add to the required drive voltage. Finally, at the bottom is a summary of characteristic contact resistance, contact power loss, and contact area for each of the three contactor types.

Fig. 9 - Hollow Cathode Operation (Inner region): A cathode to anode/keeper discharge current (not shown) results in a high density core volume of weakly ionized, highly collisional plasma freely expanding into the surrounding vacuum (while its center of mass moves away from the HC orifice at sonic-choked flow exit velocity  $U$ ). At large distances this becomes an expanding spherical cloud of low density, collisionless plasma. We model this as spherical expansion from a uniform "source region" of radius  $R_0$  inside of which collisional (gas) dynamics maintain equilibrium, through a transition region of complex dynamics, to a series of expanding spherical shells of low density collisionless plasma extending to some distant radius where

they either merge with the ionosphere or become distorted by outside forces (magnetic field, etc.). Conservation of particles, plus estimates that  $\dot{R}$  stays in the range of sonic to "Bohm" velocities yields an estimated total current conduction capacity of 10- 1,000 amperes. This might be increased if electron heating or sheath ionization occurs. To first order, the current can flow in either direction, from inner to outer boundary as frequently observed, or from outer to inner if the outer boundary is a source of electrons (probably true for a surrounding plasma, harder to simulate inside a laboratory chamber). The "ion current" required from the hollow cathode source is established by the loss rate from the "plasma ball" ( $\dot{R} \times n \times R^2$ ), independent of actual tether current being drawn thru the system.

Fig. 10 - Hollow Cathode Operation (Outer Region): The expanding plasma cloud, radial velocity now assumed constant, falls off in density as  $R^{-2}$  until it is less than (lost in) the surrounding ionosphere. With no tether current through it, it will assume some equilibrium voltage distribution such that thermal current densities balance against the density gradient/thermal current gradient effects. This probably requires  $\Delta\phi$  of a few times  $kT$  for every two orders of magnitude  $\Delta n$ . This is an equilibrium, with no net current flow. Any attempt to upset this equilibrium by putting either positive or negative voltage on the (hollow cathode source) end of the tether will result in exponential increases in current flow to oppose it, up to the limit where the tether current begins to dominate the thermal current densities/equilibrium conditions. Using the inner

boundary condition of  $N_0 = 10^{12}/\text{cc}$  at  $R_0 = 10$  cm, this limit would be well in excess of 100 amperes at voltage drops less than 10 volts. If the magnetic field acts to impede these currents, the Bohm Diffusion equation would indicate that either electron heating or additional ionization of the neutrals would be required to allow conduction, and either condition could be satisfied by several mechanisms at relatively small additional voltage drop. Also, if magnetic connection occurs it will sweep away the plasma at orbital velocity, resulting in a higher source current required to sustain the plasma cloud. This will be delayed in practice by EXB drifts in the charge separation field set up in the finite width of plasma, which will tend to cause the plasma to continue moving with the source. The effective boundary of the plasma cloud can be defined at  $R = 100$  m for a  $10^6/\text{cc}$  surrounding ionosphere, expanding to  $R = 1\text{km}$  for a  $10^4/\text{cc}$  ionosphere. Beyond this radius the ambient thermal current densities exceed those of the hollow cathode cloud and conduction becomes that of the ionosphere, rather than that of the hollow cathode. The plasmas adjust to each other, no changes in tether operation (accelerating voltage, discharge current, etc.) are needed.

Fig. 12 - Reference curve used in design studies to estimate hollow cathode power required versus maximum tether operation current (power for heaters, discharge current and extraction voltage). Verification of this curve by experiment data on orbit is a critical issue for present and future applications studies.

$$\text{Power used} = 100 + 50I \text{ (watts)}$$

Fig. 13 - Plot of tether operating current versus power consumed in

operation, using PMG concept with hollow cathodes compared with existing electron guns (based on pervience of existing SEPAC and proposed TSS core equipment guns, extrapolated beyond 1 amp maximum planned operation).

Fig. 14 - A more general treatment of tether current contactor performance than fig. 13, plotting voltage drop across contact sheath/beam at each end of tether vs. tether current (to get power loss, multiply by I and add heater and controler power). The PMG hollow cathode design curve (from fig. 12 and fig. 13) is straight solid line at 25V. Actual data values measured in lab fall roughly along dashed line below that (see fig. 30). The fig. 13 curves for SEPAC and TSS guns are in upper left corner. Curves for other devices and/or other assumptions fall everywhere in between:

- 1) TSS satellite, space charge limited electron collection at  $10^6/cc$   
     ⊙ = no magnetic field    ⊗ = Parker & Murphy model
- 2) 30cm Kaufman thruster with electron beam (-I, only)
- 3) 30cm Kaufman thruster with ion beam (+I, only)
- 4) S-cubed model for hollow cathode, using NASCAP
- 5) PMG model, with electron heating/Bohm Diffusion @ (a)  $10^4/cc$ , (b)  $10^6/cc$
- 6) PMG model, with Parker and Murphy diffusion model @ (a)  $10^4/cc$ , (b)  $10^6/cc$

Fig. 15 - Insulation requirements and drag area in lower orbits strongly force moderate power (20KW-200KW) tethers toward maximum lengths of 10-20 km, if normal insulation thickness standards (100 volts/mil) are applied. Use of very highly stressed (5KV/mil) insulation could avoid part of this, but probably has severe problems with



pinhole leakage/breakdown phenomena at high voltage in a plasma environment.

Fig. 16 - Nature is hostile toward long, thin tethers. Electrically, 100 km of #12 wire weighs 900 kg and performs as efficiently as 10 km of #2 wire, which also weighs 900 kg. However, the 100 km wire (2 mm dia) can expect to be cut 15-20 times per year by meteoroids or debris, while the 10 km wire (6.5 mm dia) can expect 4-8 years between penetrating impacts. At this size, debris particles are the primary hazard. The debris problem is reduced at lower altitudes due to reduced dwell times in denser atmosphere. The Megawatt PMG Reference System (20km x 2cm dia) could expect 30 years between penetrations, in a 400 km orbit.

### III. Massive Tether Dynamics

The basic PMG design involves a massive tether cable (or pair of cables deployed one up and one down) with little or no satellite mass at the far end(s). Deployment is permanent for most applications, therefore control law reeling for rapid deployment/retrieval is unnecessary. The IXB forces are dominant, leading to use of IXB time phasing, rather than tether reeling, for control. Special applications may benefit from use of secondary "ballast" tethers attached (in place of satellites) at the PMG far ends, but normally any weight that could be added to end mass to increase PMG tether tension/stability is more beneficial if distributed along the wire as a heavier conductor, thereby increasing electrical efficiency.

The dynamic behavior of the massive PMG tethers is distinctly different from the TSS configuration.

- Fig. 17 - Summary of dominant factors in massive tether dynamics for PMG applications.
- Fig. 18 - Illustration of massive tether (no satellite) under strong IXB (thrust) force disturbance; superimposed on simple massless tether model often used for discussions of tether fundamentals. Note the curvature of tether cable, location of center of gravity (c.g.) displaced from host spacecraft, relation between tether tension/deflection angle at c.g. and net acceleration force transmitted to c.g./spacecraft ( $T \sin \alpha = F$ ).
- Fig. 19 - Derivation of equations providing analytic approximation to two dimensional motion of massive tether.  $T(z)$  is tension in tether and  $\alpha$  is deflection from vertical (first solution is for  $T(z)$  and  $\sin \alpha$  if tether is at equilibrium),  $X_{tt}$  is acceleration at non-equilibrium point.
- Fig. 20 - General solution requires computer modeling and has not yet been completely solved, but GTOSS provides useful approximation with wide applicability. Figure displays orbit, coordinates, and general configuration (model) used in following solutions for 100KW PMG, with optional "ballast" tether as shown and day/night cycle reversals of current to excite the critical out-of-plane libration resonant at half orbital period.
- Fig. 21 - Results for 10,000 lb, 65,000 foot PMG system operating at 100 KW with 50/50 day-night power cycle (power storage/power generation, to replace battery system used with large solar array). This is the most critical situation for 2:1 resonance with the out-of-plane libration, and the libration is seen here to grow rapidly beyond 10 degrees by orbit #3, exceeding 30 degrees during orbit #5. Notice

the effect on tether voltage (EMF), which is seen to vary with magnetic field in the "normal" manner during orbit #3, between roughly 3,000 to 4,500 volts. By orbit #5, the tether is swinging so far away from the vertical that it becomes nearly parallel to the field at 30°N latitude and the EMF drops to only 400 volts! At this point the tether has become essentially useless, as well as nearly out of control. Such operation must be avoided.

Fig. 22 - Proposed simple method to avoid problem in fig. 21, other than by suspending or reducing day/night operations. This is also useful for the unrelated, but equally troublesome problem of variable angular rates in eccentric orbits - such as would occur during electrodynamic boost of a transfer orbit's apogee during perigee passes through low altitude. (A tether reel controller could be placed at either end of the "ballast" tether to further strengthen the control capabilities, in place of the ballast mass or where electric power is most easily provided by the PMG. The following calculations indicate this is not necessary. For any given mission, trade-offs between total mass and complexity/reliability of operation should be studied.)

Fig. 23 - Comparison between rate of increase in out-of-plane librations between (a) worst case (50/50 power cycle), (b) real world day/night power storage/generation (65/35 power cycle, thrust at 53KW during day, power generation at 100 KW during night) with "bare" PMG, and (c) same as (b) except stabilized by 1,000 lb passive ballast tether (no reeling). No attempt to reduce libration by selective phasing of IXB loading was made in these runs (i.e., "worst case" assumption, that power load could not be

adjusted at all to allow use of "electrodynamic control law"). The problem is substantially reduced in case (b), but definitely still present. In case (c), resonance appears to be broken, problem solved (long term runs would be needed to verify that secondary resonance terms don't eventually show up, but only if long term power budget stayed "locked in" to resonance condition). Therefore, no need for complex tether reeling mechanism is seen for this extreme case.

Fig. 24 - Corresponding in-plane libration (which is necessary factor in production of power or thrust via electrodynamic tethers on a single host spacecraft) for the three cases in fig. 23. Libration appears well behaved in all three cases.

Fig. 25 - Relative libration behavior of massive PMG cable end and ballast mass, showing relative phase shifts producing damping effect and disruption of phase resonance conditions.

#### IV. Jupiter Mission

In 16 years it will be 2001, and some time ago many of us were given a vivid impression that this might be the year man goes to Jupiter. Maybe the movie will not prove exactly accurate about the date, purpose, spacecraft, and crew; but Jupiter does provide a very good focus for considering the possible uses of electrodynamic tethers outside the "mundane" near earth applications for power, propulsion and research discussed so far. Jupiter has a very strong magnetic field (4 Gauss near the surface) providing a very extensive magnetosphere (extending more than a million miles), ideal conditions for electrodynamic tethers. While electrodynamic effects become too small for practical use with existing tether materials within a few thousand kilometers

of the earth, they remain strong well beyond 300,000 km at Jupiter. The Jupiter magnetoplasma may be rather low density, but the hollow cathode plasma cloud can probably expand to adjust for this. In any case Jupiter provides a good example to examine some additional capabilities of the PMG tether, and is the most likely place outside low earth orbit to benefit from, or require the use of, electrodynamic tethers for its future exploration and development.

Fig. 26 - Plot of orbit energy within the Jupiter system, as shown yesterday during my general presentation to the opening session. The intense gravity makes it extremely difficult to get around within the inner system by use of rockets, either chemical or electric, for orbit transfer delta-V. The energy required to achieve Low Jupiter Orbit (LJO) is much more than required to get to Jupiter from the Earth. Expressed as millions of joules per kilogram (Mj/kg) or kilowatt hours per kg (KWHR/kg) it becomes clear that these energy levels are not practical for rocket propulsion, but well within the theoretical capabilities of electrodynamic tether propulsion. Also plotted (in green) is the velocity for circular orbit and (dashed green) corotational velocity of the magnetoplasma. The vertical scale reads in km/sec for the velocity plots. A very significant difference from the Earth's situation is that corotation becomes important, even dominant, relatively close to the planet at  $2 R_J$  (about 70,000 km above the surface) where electrodynamic tether forces are still very strong. (At geosynchronous orbit, GEO, the magnetic field is too weak to be useful without a superconducting tether.)

Fig. 27 - The induced voltage for a radially aligned tether in circular orbit

versus distance is shown, under two different assumptions. The solid blue line ignores corotation (assumes the velocity in VXB is orbital velocity, and the velocity of the Jupiter "ionosphere" in return circuit is zero). The green line assumes 100% corotation. As a result, VXB goes thru zero, becoming negative (dashed green line) beyond 2.2 Jupiter radii. This is a fundamental difference. In this region, tether power generation no longer produces drag that decelerates the spacecraft toward lower orbits, but instead produces thrust that accelerates it toward higher orbit. Near 2.2  $R_J$ , the VXB induced voltage in the tether is rather low, while the IXB thrust force is still large. At exactly the corotation radius, the power required to drive a current against the tether EMF is zero while the thrust (per ampere) is still greater than that available in LEO at a cost of 8KW/newton! This is not a paradox, or a perpetual motion machine. It is a simple result of the fact that the electrodynamic tether couples to the frame of motion of the magnetoplasma surrounding it. If the rest frame of that magnetoplasma is not the same as the gravitational rest frame of its orbit, energy is naturally transferred. Beyond 2.2 Jovian radii in a corotating magnetosphere, IXB drag does just that, it drags the tether along toward the corotational velocity as long as the magnetosphere remains firmly coupled to the rotation of the planet, or toward whatever intermediate velocity may be the effective rest frame of the magnetoplasma! The same phenomena should be seen in the solar wind (where  $V = 400$  km/sec is very high compared to orbit velocity around the sun, and orbital velocity is a negligible term for an "Alfven Engine") or in LEO (where

corotation is about .5 km/sec, much less than orbit velocity - would produce a small, but noticeable difference between prograde and retrograde equatorial orbits). If the condition of corotation is satisfied, the Jupiter Synchronous Orbit (JSO) is a unique point in the solar system. A space station (space factory, or space city) located at JSO would be anchored stationary with respect to the Jupiter magnetosphere. By deploying a pair of tethers, one up into higher velocity magnetoplasma and one down into lower velocity magnetoplasma, both tethers could be used to produce power while providing balanced (off-setting) drag/thrust forces on the space station. This particular space station could then consume all the tether generated power it wanted and never have to reboost (or reloader, in the case of solar orbiting "Alfven Engines" or spacecraft higher than JSO) its orbit. Somewhat analogous to how a hydroelectric plant gets "free" power as long as rain keeps falling uphill from its location, the Jupiter corotating station can get "free" power from the planet's rotational energy as long as the planet continues to drive a corotational magnetosphere.

Fig. 28 - Comparison of tether tension and thrust/drag force, for a gravity gradient stabilized tether system in circular orbits around Jupiter. The low density of Jupiter causes the gravity gradient force to be relatively small, even for a very long PMG tether. This would limit operation to a small fraction of peak available power (the PMG assumed for this graph would be capable of 2 Megawatts in LEO, 200 Megawatts in LJO), unless additional stabilizing force is provided. This is readily done. Jupiter based PMG's would either use a long "anchor" of low mass (see "ballast" tether in fig. 20,

22) to maintain gravity gradient alignment, or would use several short PMG's arranged in a spinning configuration for centrifugal force stabilization.

#### V. Demonstration Experiments

Obviously, the PMG electrodynamic tether is a very powerful device; if and only if the hollow cathode current coupling, as well as the ionospheric plasma return current conductance common to all electrodynamic tether concepts, works as it is assumed in these studies. Confirmation of this assumption, even to order of magnitude, is critical to the validity of all the important results discussed today. Flight of a hollow cathode experiment on TSS, as well as detailed scientific study of the TSS electrodynamic interactions, is vital.

It is also important to verify, as soon as possible, the current coupling performance of a hollow cathode system in LEO to confirm our present emphasis on PMG type tether designs, rather than passive balloon and/or electron gun based concepts. Laboratory tests have been performed that indicate the model is correct, at least for electron emission, but extrapolation of plasma chamber test data to space plasma conditions is uncertain.

Fig. 29 - A small "experiment of opportunity" is being built at NASA-JSC, named PMG/POF (Plasma Motor-Generator/Proof of Function) Experiment. Scheduled for Space Shuttle flight on the Hitchhiker G carrier's second flight (HHG-2) in 1986, it is designed to measure the current/voltage characteristics of a pair of hollow cathode devices operating at 200 meter separation in low earth orbit.

Fig. 30 - Calibration data taken at Colorado State University, using a prototype hollow cathode assembly (HCA) built for PMG/POF.

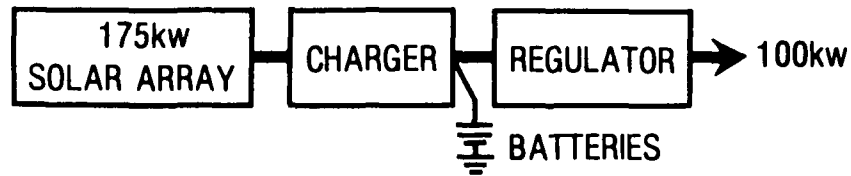


Measured values of electron emission and electron collection currents (electron collection via "ion production" plasma, lower curve). Electron collection appears to be limited primarily by sheath impedances around the hot filament source.

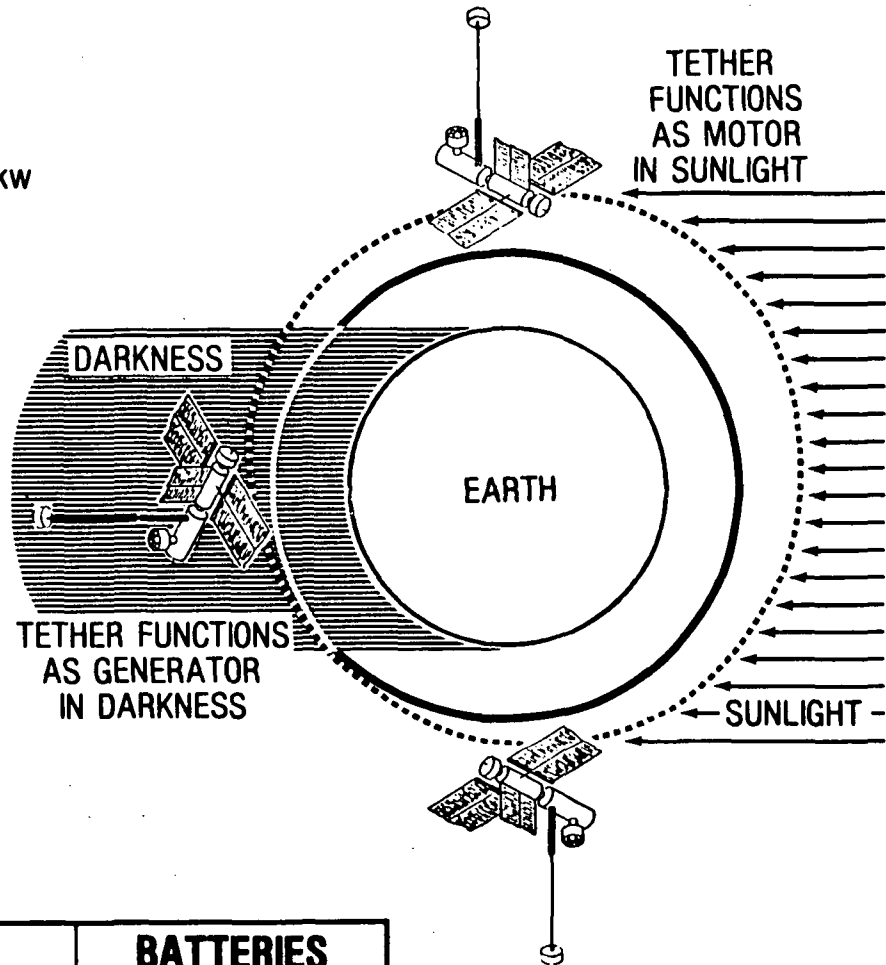
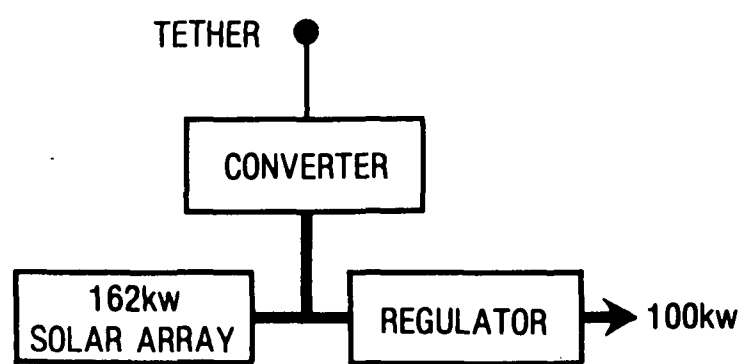
Fig. 31 - Calibration data taken on same prototype HCA, ion production (plasma source volume) versus cathode/anode discharge power at various neutral gas input rates (1 to 18 standard cubic centimeters per minute, Xenon gas). Test results directly demonstrated electron emission current exceeding 1.5 amperes, electron collection current exceeding .15 ampere. Reasonable extrapolation of this data indicates ultimate current capacity of this system exceeding several amperes, emission or collection.

# ELECTRODYNAMIC TETHER ENERGY STORAGE

## SOLAR ARRAY – BATTERIES



## SOLAR ARRAY – TETHER

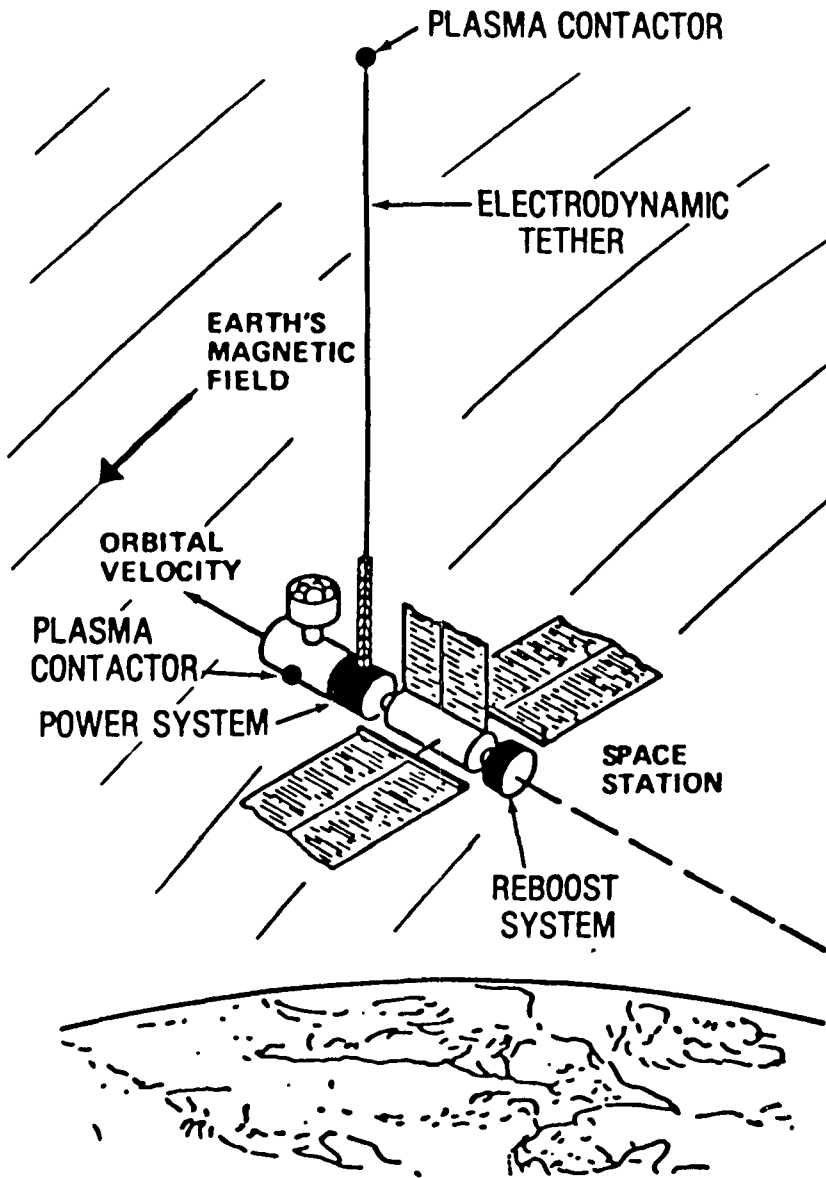


564

	TETHER	BATTERIES
● WEIGHT COMPARISON	15K LBS	24K LBS
● HEAT REJECTION REQMTS	40,000 BTU	75,000 BTU
● DEEP DISCHARGE CAPACITY	57,000 KWH	50 KWH

Figure 1

# BACKUP TO SPACE STATION PRIME POWER AND REBOOST SYSTEMS



## POWER SYSTEM FAILURE

- USE TETHER AS GENERATOR
- MAKEUP INCREASED DRAG WITH REBOOST MODULE
- 3 MONTHS AT 10kw FROM 9,000lbs HYDRAZINE

## REBOOST MODULE FAILURE

- USE TETHER AS MOTOR FOR REBOOST
- USE POWER FROM SOLAR ARRAY SYSTEM
- SPACE STATION DRAG MAKEUP REQUIRES ONLY 5-8 kw OF SOLAR ARRAY POWER

Figure 2

" 200 kW " PMG

INITIAL OPS @ 100 kW

RATED OPS @ 200 kW

PEAK/EMERGENCY OPS @ 500 - 1,000 kW

PRIMARY TRADE-OFF :  $I^2R$  POWER LOSSES vs TETHER MASS

TENSION LOADS VERY LOW vs CABLE STRENGTH (AL WIRE)

TEFLON INSULATION ADEQUATE @ 10-20 KM TETHER LENGTH (2-4KV)

(IF USE LOW CURRENT/HIGH VOLTAGE TETHER, INSULATION HEAVY & UNCERTAIN)

NO TETHER REELING FOR CONTROL

IXB PHASING PRIMARY CONTROL TECHNIQUE

ADDED STABILITY AVAILABLE USING "BALLAST" TETHER EXTENSION

"MASSLESS" KEVLAR TETHER W 10% END MASS

COULD STUDY "KEEL CONTROLLER" LOCATED @ FAR END

PMG - 200 KW REFERENCE SYSTEM

TETHER LENGTH	20 KM (10 UP+10 DN)	WORKING TENSION	42 N
NOMINAL VOLTAGE	4 KV	WORKING ANGLE	17 DEG
RATED POWER	200 KW	RATED THRUST	25 N
PEAK POWER	500 KW	PEAK THRUST	>100 N

CONDUCTOR	#00 AWG ALUMINUM WIRE DIAMETER 9.3 MM @ 20°C RESISTANCE 8.4 OHMS @ 20°C 7.7 OHMS @ 0°C 7.1 OHMS @ -20°C	3640 KG
INSULATION	0.5 MM TEFLON (100 VOLTS/MIL)	278 KG
FAR END MASS	50 AMP HOLLOW CATHODE ASS'Y (INCLUDING ELECTRONICS & CONTROL)	25 KG
TETHER CONTROLLER	ELECTRONICS & MISC. HDWR. (POWER DISSIPATION LOSSES @1% = 2 KW)	94 KG
ARGON SUPPLY & CONTINGENCY RESERVE		<u>163 KG</u>
<u>TOTAL</u>		<u>4,200 KG</u>

TETHER DYNAMICS CONTROL	PASSIVE, IXB PHASING	
TETHER CURRENT/POWER CONTROL	DC IMPEDANCE MATCHING	
TETHER OUTSIDE DIAMETER	10.3 MM	
TETHER BALLISTIC DRAG AREA	206 SQ METERS	
DRAG FORCE @ 10 <sup>-11</sup> KG/M <sup>3</sup>	.12 N	.96 KW
(300 KM 1976 USSA-400 KM SOLAR MAX)		
I R LOSSES @ 200 KW		19.25 KW
HOLLOW CATHODE POWER		2.50 KW
IONOSPHERIC LOSS @ 50 AMP		<u>1.25 KW</u>
TOTAL PRIMARY LOSSES		23.96 KW
EFFICIENCY	ELECTRIC (177 KW NET @ 50 AMP/200 KW)	88.5%
	OVERALL (201 MECH. TO 177 ELEC. KW)	88.1%
INCLUDING CONTROLLER/POWER PROCESSER LOSSES @ 1%		<u>2.00 KW</u>
TOTAL (NET POWER OUT 175.0 KW)		25.96 KW
FINAL EFFICIENCY	ELECTRIC = 87.5%	OVERALL = 87.1%

PMG - MEGAWATT REFERENCE SYSTEM

TETHER LENGTH	20 KM (10 UP+10 DN)	WORKING TENSION	190 N
NOMINAL VOLTAGE	4 KV	WORKING ANGLE	10 DEG
RATED POWER	500 KW	RATED THRUST	65 N
PEAK POWER	>2 MW	PEAK THRUST	>400 N

CONDUCTOR	2 CM ALUMINUM WIRE DIAMETER 20.0 MM @ 20°C RESISTANCE 1.68 OHMS @ 20°C 1.54 OHMS @ 0°C 1.42 OHMS @ -20°C	17,860 KG
INSULATION	0.5 MM TEFLON (100 VOLTS/MIL)	580 KG
FAR END MASS	125 AMP HOLLOW CATHODE ASS'Y (INCLUDING ELECTRONICS & CONTROL)	50 KG
TETHER CONTROLLER	ELECTRONICS & MISC. HWWR. (POWER DISSIPATION LOSSES @1% = 5 KW)	120 KG
ARGON SUPPLY & CONTINGENCY RESERVE		<u>290 KG</u>
<b>TOTAL</b>		<b><u>19,000 KG</u></b>

TETHER DYNAMICS CONTROL	PASSIVE, IXB PHASING	
TETHER CURRENT/POWER CONTROL	DC IMPEDANCE MATCHING	
TETHER OUTSIDE DIAMETER	21.0 MM	
TETHER BALLISTIC DRAG AREA	420 SQ METERS	
	-11      3	
DRAG FORCE @ 10 <sup>2</sup> KG/M	.25 N	2.0 KW
(300 KM 1976 USSA-400 KM SOLAR MAX)		
I R LOSSES @ 500 KW		<u>24.1 KW</u>
HOLLOW CATHODE POWER		5.0 KW
IONOSPHERIC LOSS @ 125 AMP		<u>7.8 KW</u>
TOTAL PRIMARY LOSSES		36.9 KW
EFFICIENCY	ELECTRIC (463.1 KW NET @ 500 KW)	92.6%
	OVERALL (502 MECH. TO 463 ELEC. KW)	92.3%
INCLUDING CONTROLLER/POWER PROCESSER LOSSES @ 1%		<u>5.0 KW</u>
TOTAL (NET POWER OUT 458.1 KW)		41.9 KW
FINAL EFFICIENCY	ELECTRIC = 91.6%	OVERALL = 91.3%

ELECTRODYNAMIC TETHER  
RECOMMENDED APPLICATIONS

I. THRUST - USE WITH SOLAR ARRAYS IN LOW EARTH ORBIT TO OFFSET DRAG

100 KG SYSTEM PRODUCING .1 NEWTON THRUST

8 KW/N ELECTRIC POWER CONSUMPTION = .8KW

ELIMINATES DELTA-V FUEL REQUIRED: >1,000 KG/YR

KEEP 100 KW SOLAR ARRAY @ SPACE STATION ORBIT

INCREASE TO 200 KG SYSTEM @ 1-2 N THRUST

KEEP SPACE STATION + 100KW ARRAY IN <300 KM ORBIT ALTITUDE

NO ORBIT MAINT. FUEL REQUIRED; CONSUMABLES = < 60 KG/YR (ARGON)

USES 10-15 KW FROM 100 KW AVAILABLE

II. THRUST - USE FOR ORBITAL MANUEVERING PROPULSION

2,000 KG SYSTEM (PLUS 80 KW POWER SUPPLY: SOLAR, NUCLEAR, WHAT-EVER)

10 NEWTON THRUST - CONTINUOUS AS LONG AS POWER AVAILABLE

ALTITUDE CHANGE

7 KM/DAY - 200,000 KG (SPACE STATION)

30 KM/DAY - 50,000 KG (PLATFORM)

150 KM/DAY - 10,000 KG (FREE-FLYER)

TOTAL IMPULSE: 864,000 N-SEC/DAY (194,000 LB-SEC/DAY)

17 M/SEC/DAY - 50,000 KG (PLATFORM)

86 M/SEC/DAY - 10,000 KG (FREE-FLYER, OMV, OR "TUG")

ORBIT PLANE CHANGE: 30 DEGREE IN 6 MONTHS MAY BE POSSIBLE

"FLY" ENTIRE SPACE STATION DOWN TO 200-250 KM ALTITUDE & MAINTAIN

GROWTH VERSION: 200 N @ 1.6 MW, 20,000 KG + POWER SUPPLY

III. POWER STORAGE - 100KW SOLAR ARRAY SYSTEM

+ 2,000 KG REVERSIBLE MOTOR/GENERATOR TETHER SYSTEM

60 KW THRUST DURING DAY (POWER STORAGE AS ORBIT ENERGY)

100 KW POWER GENERATION DURING DARK

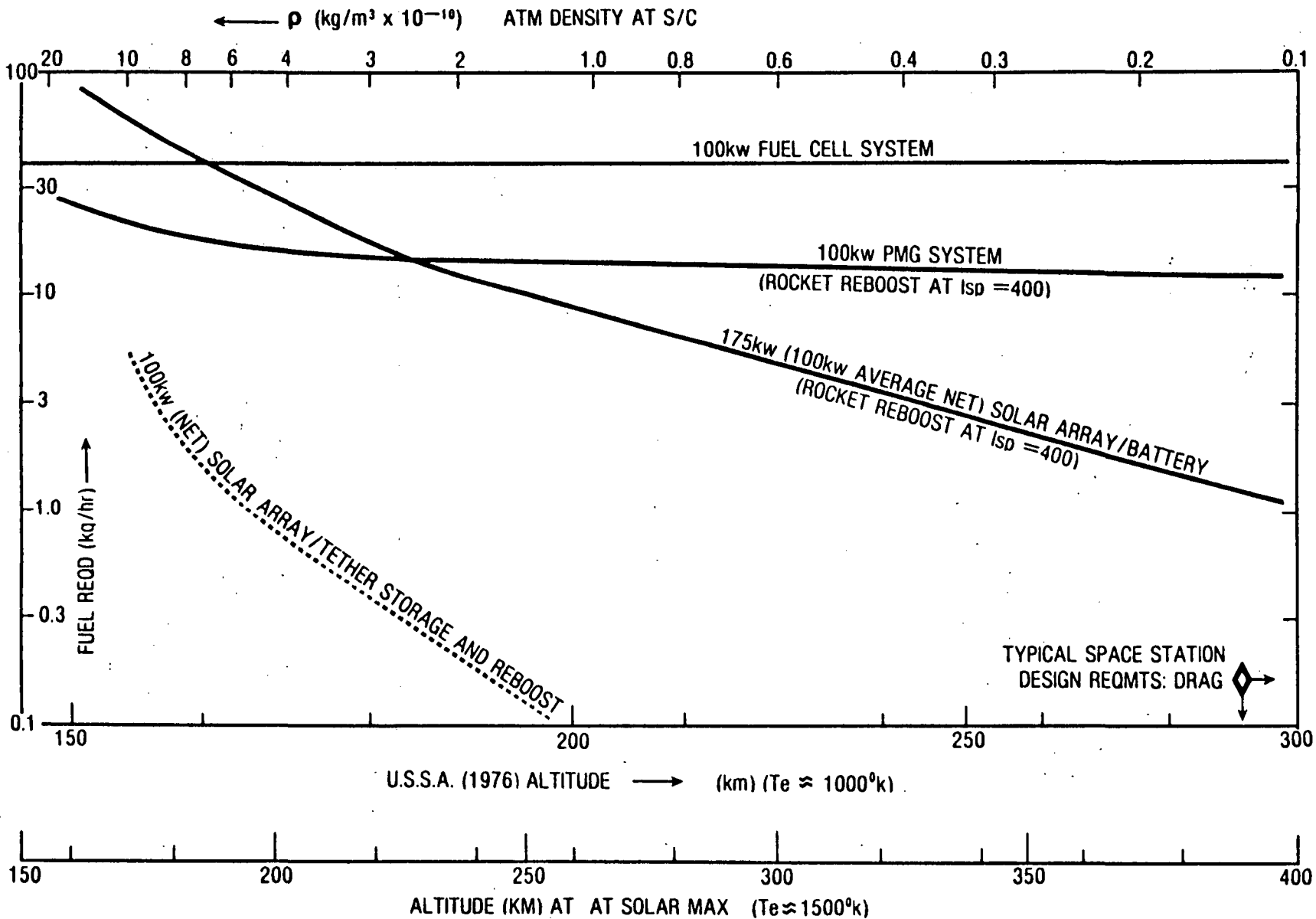
TOTAL SYSTEM WEIGHT 40% OF CONVENTIONAL ARRAY WITH BATTERIES

10% REDUCTION IN SOLAR ARRAY SIZE

60% REDUCTION IN POWER PROCESSING HEAT REJECTION REQUIRED

# CONSUMABLES REQUIRED VS ORBIT ALTITUDE

## 100kw NET POWER GENERATED

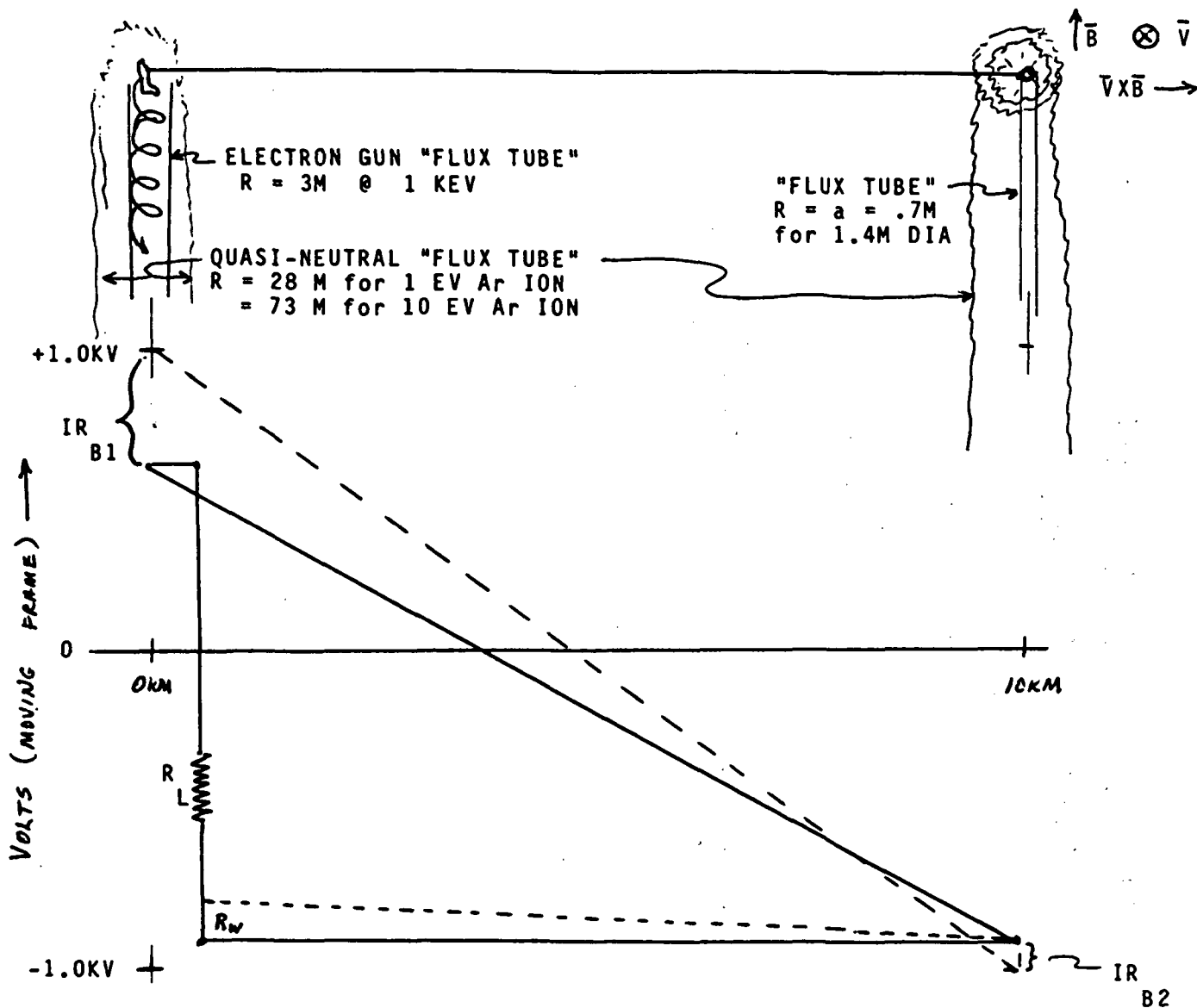


570  
C-7

Figure 7

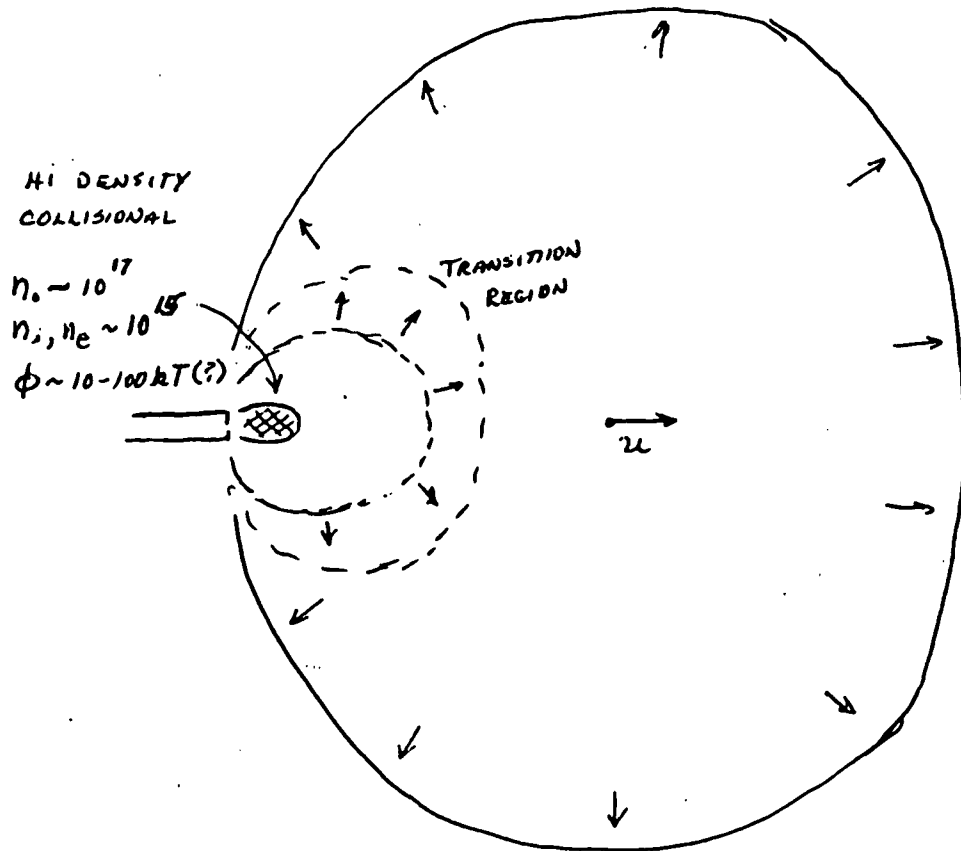


# ELECTRODYNAMIC TETHER



	PASSIVE COLLECTOR	ELECTRON GUN	HOLLOW CATHODE
R	(SCL) SHEATH	PERVIERCE	QUASI-NEUTRAL
B1	0-1,000 for +I 0-100 for -I	100-1,000 for +I infinite for -I	< 1 for +I (?)
PB1	0 watts (+DRAG)	.5 - 5 KW	100 - 300 watts
CONTACT AREA	$\frac{D^2}{4}$	20 M <sup>2</sup>	>400 M <sup>2</sup> (?)

Figure 8



w/o B field

EXPANDING SPHERE(S) w'  $u = V_0$ 

$$(\dot{R}_1) n_1 R_1^2 = n_2 R_2^2 (\dot{R}_2)$$

@ EQUILIBRIUM  $n_{i0} \sim 10^{14} \rightarrow n_{iex} \sim 10^6$ w  $\nabla\phi \Rightarrow$  RETARD ELECTRONS

(ACCEL. IONS : "BOHM CONDITION")

$$V_i \approx \sqrt{\frac{kT_e}{m_i}}$$

~~$\nabla\phi$~~   
@ ANY R,  $j_e \sim ne \sqrt{\frac{kT_e}{m_e}}$

 $\therefore$  CAN SUPPORT A CURRENT

$$I \sim 4\pi R^2 j_e = 4\pi (R^2 n) e \sqrt{\frac{kT_e}{m_e}}$$

$\uparrow$   
const.

@  $R_0 \sim 1-10 \text{ cm}$   $n_e \gtrsim 10^{12} / \text{cc}$ 

$$\therefore I = (10^4 - 10^6) V_e = 10 - 1,000 \text{ A}$$

CAN INCREASE w 1) ELECTRON HEATING

2)  $\phi > \phi_{\text{ALFVEN}} \Rightarrow$  IONIZATION  
(IN SHEATH?)

Figure 9

$$I_{\text{Bohm}} \approx e D_B \nabla n (4\pi R^2)$$

$$\approx \frac{5 \times 10^3}{R} (kT_e) \frac{n_0}{10^4}$$

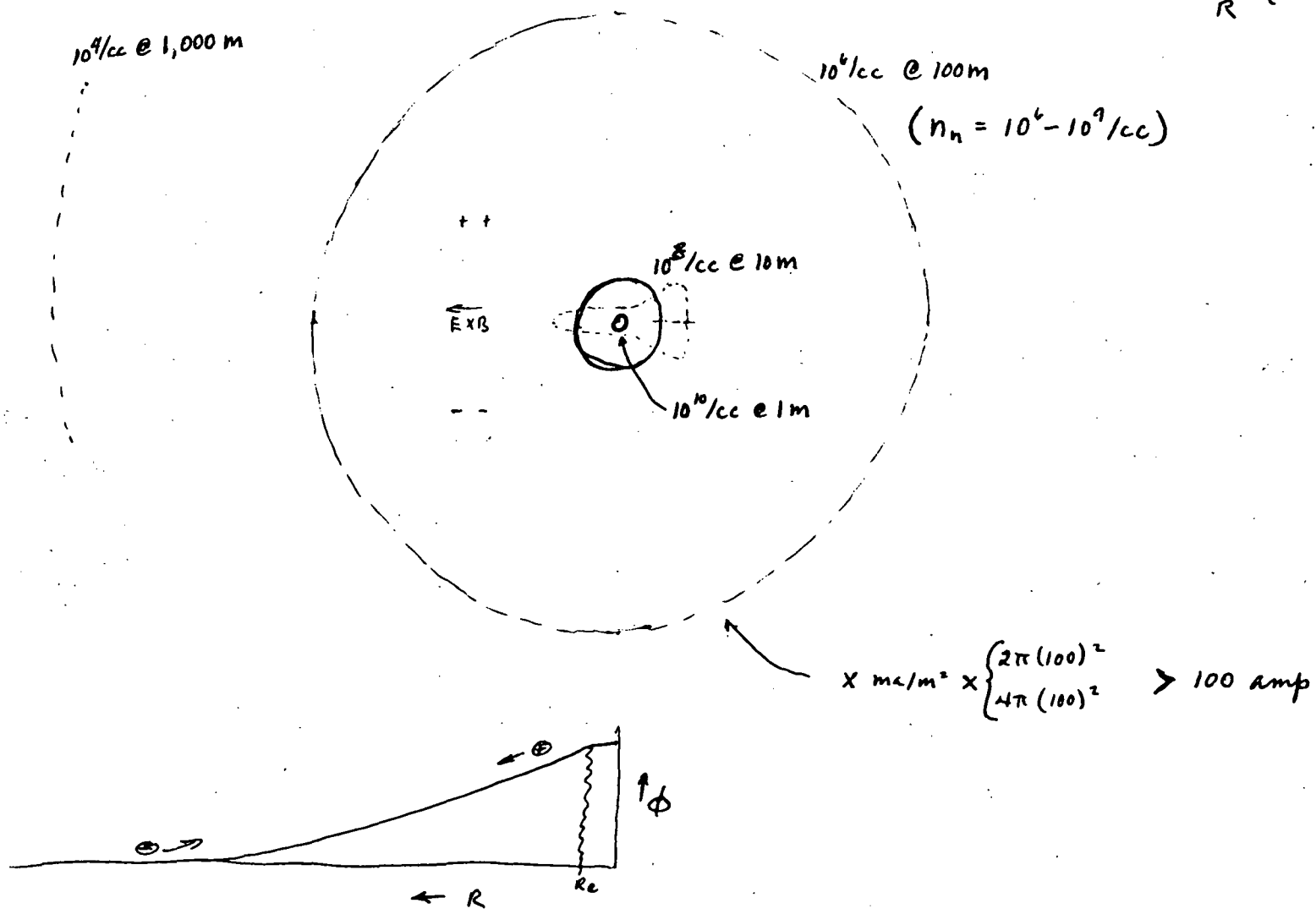


Figure 10

ORIGINAL PAGE IS  
OF POOR QUALITY

ORIGINAL PAGE IS  
OF POOR QUALITY

1123  
J. McG

HOLLOW CATHODE "NEUTRALIZER" / "PLASMA BRUSH"

POWER REQ'D vs TETHER CURRENT

$$P = 0.10 + 0.05 I \text{ (kW)}$$

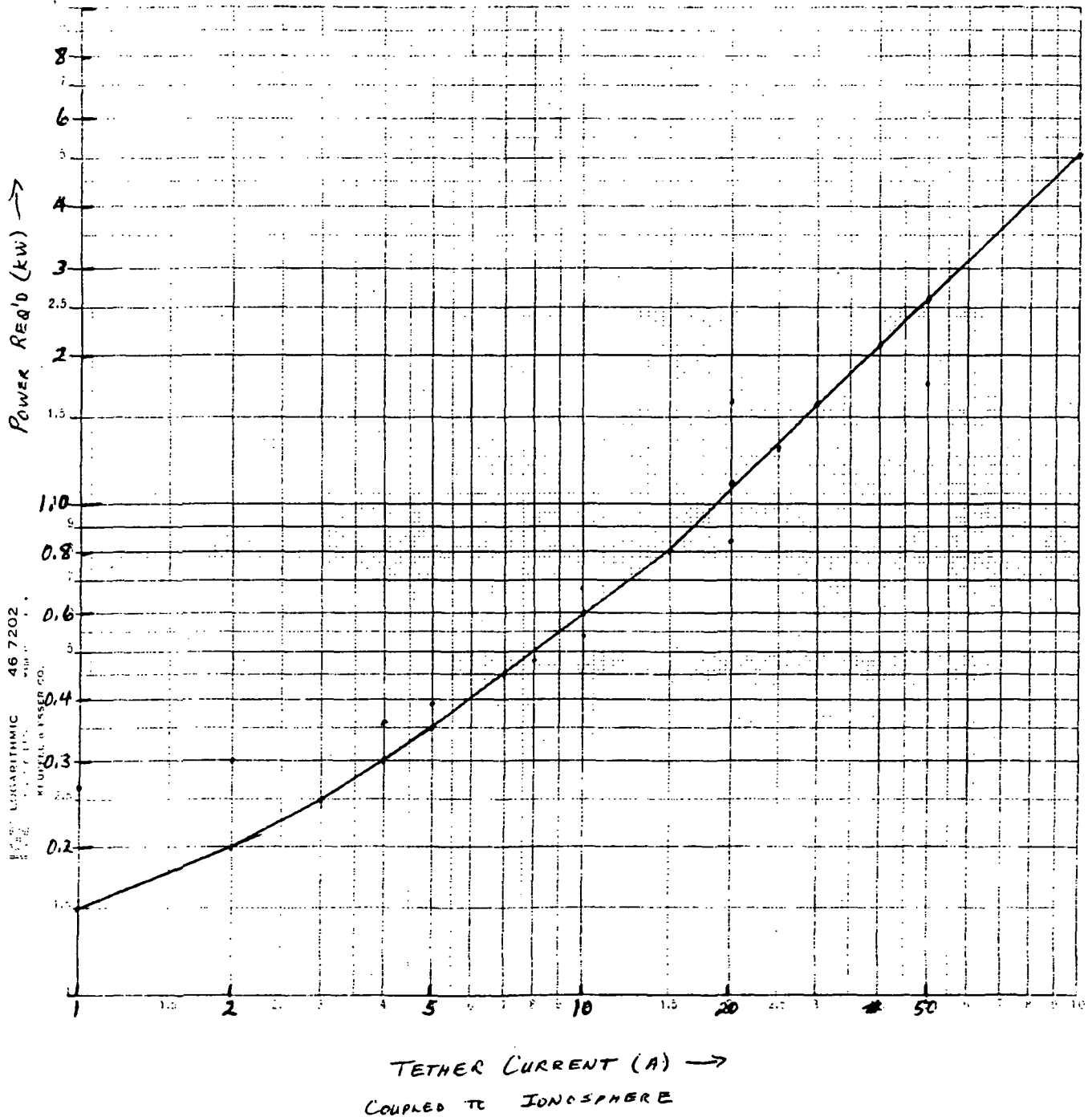


Figure 11

ORIGINAL PAGE IS  
OF POOR QUALITY

TETHER CURRENT vs POWER LOSS

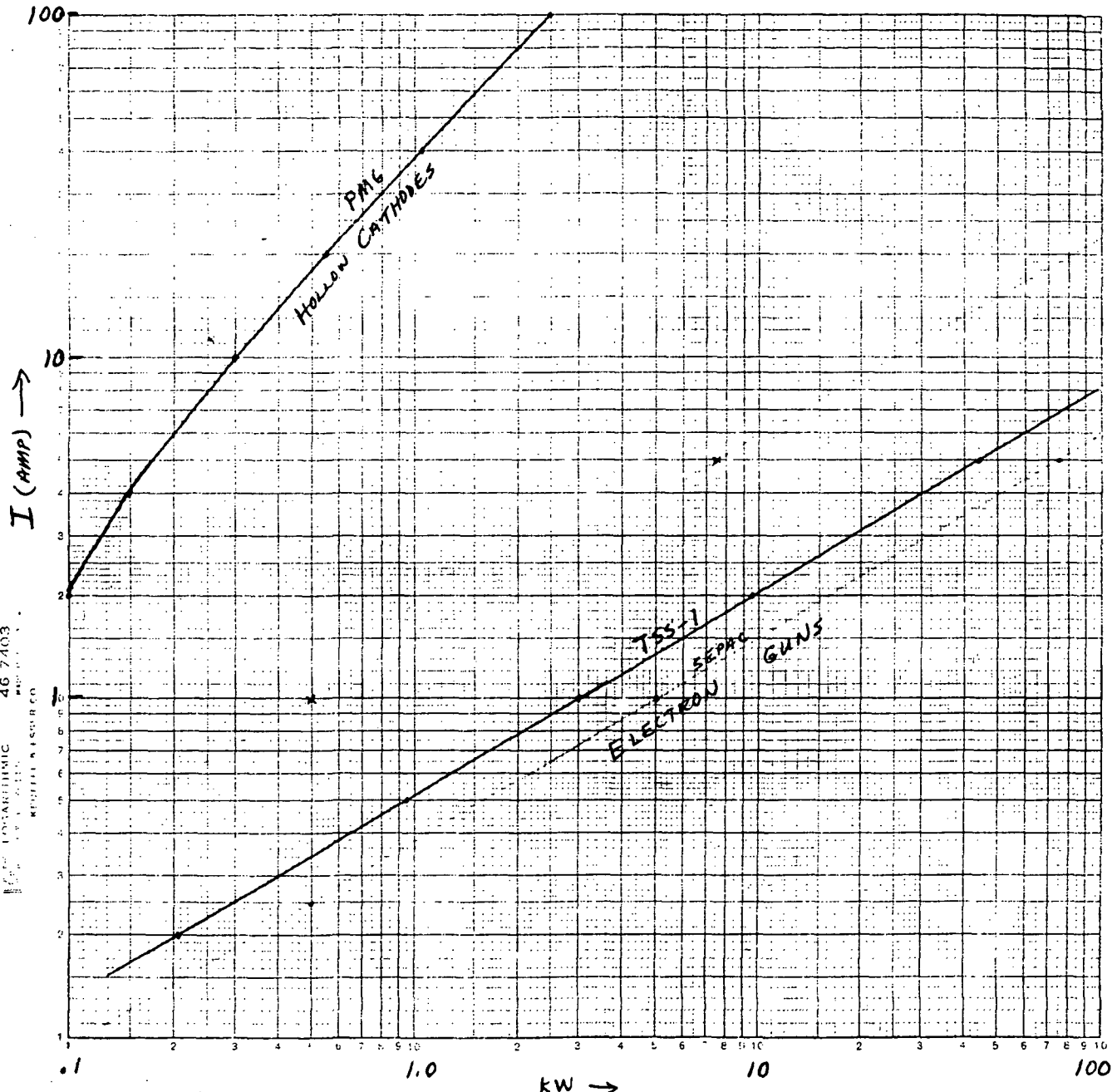


Figure 12

Power vs I

plus power req'd to create plasma, electrons, etc in absence of current

### TETHER CURRENT vs VOLTAGE LOSS

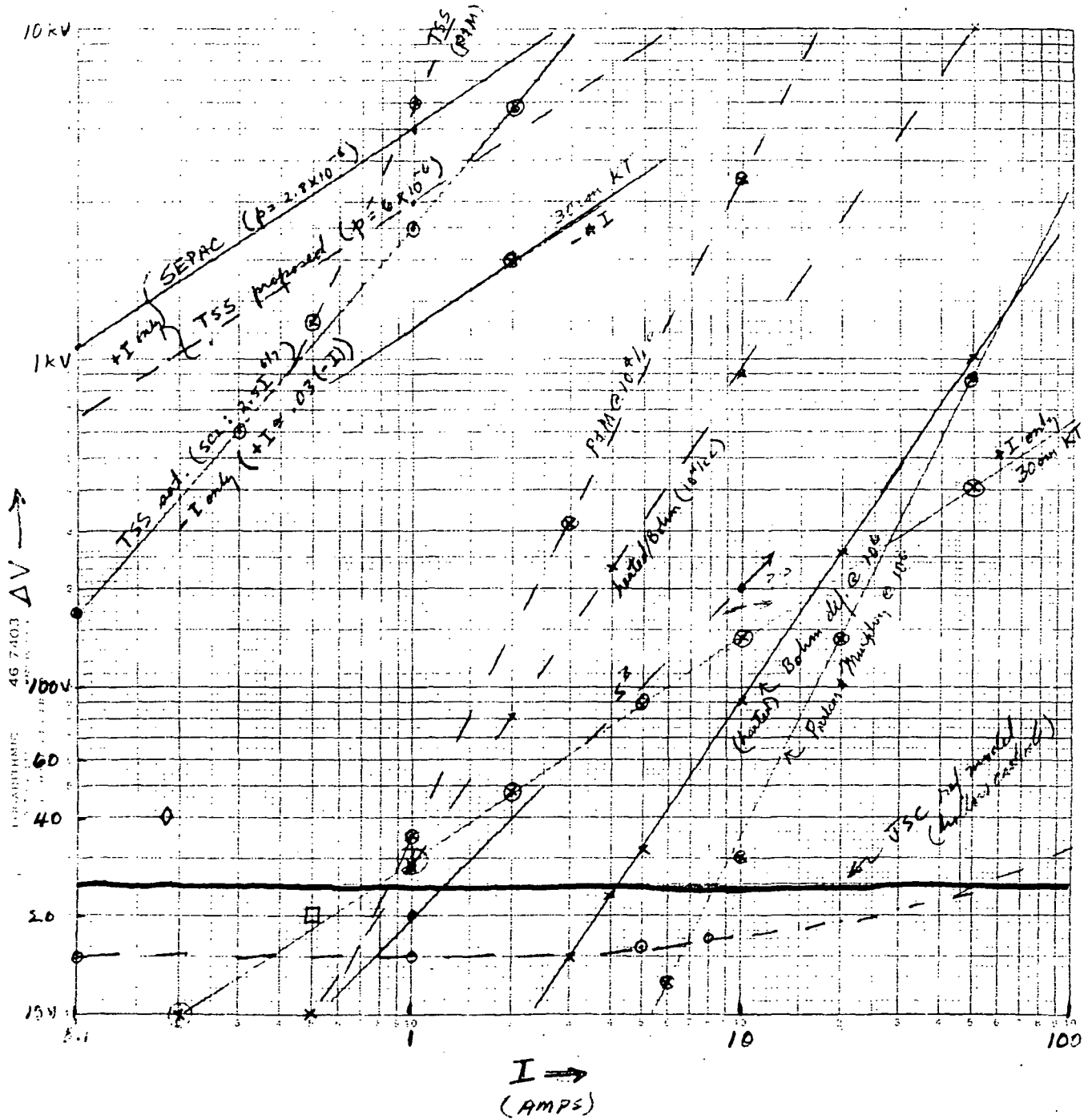
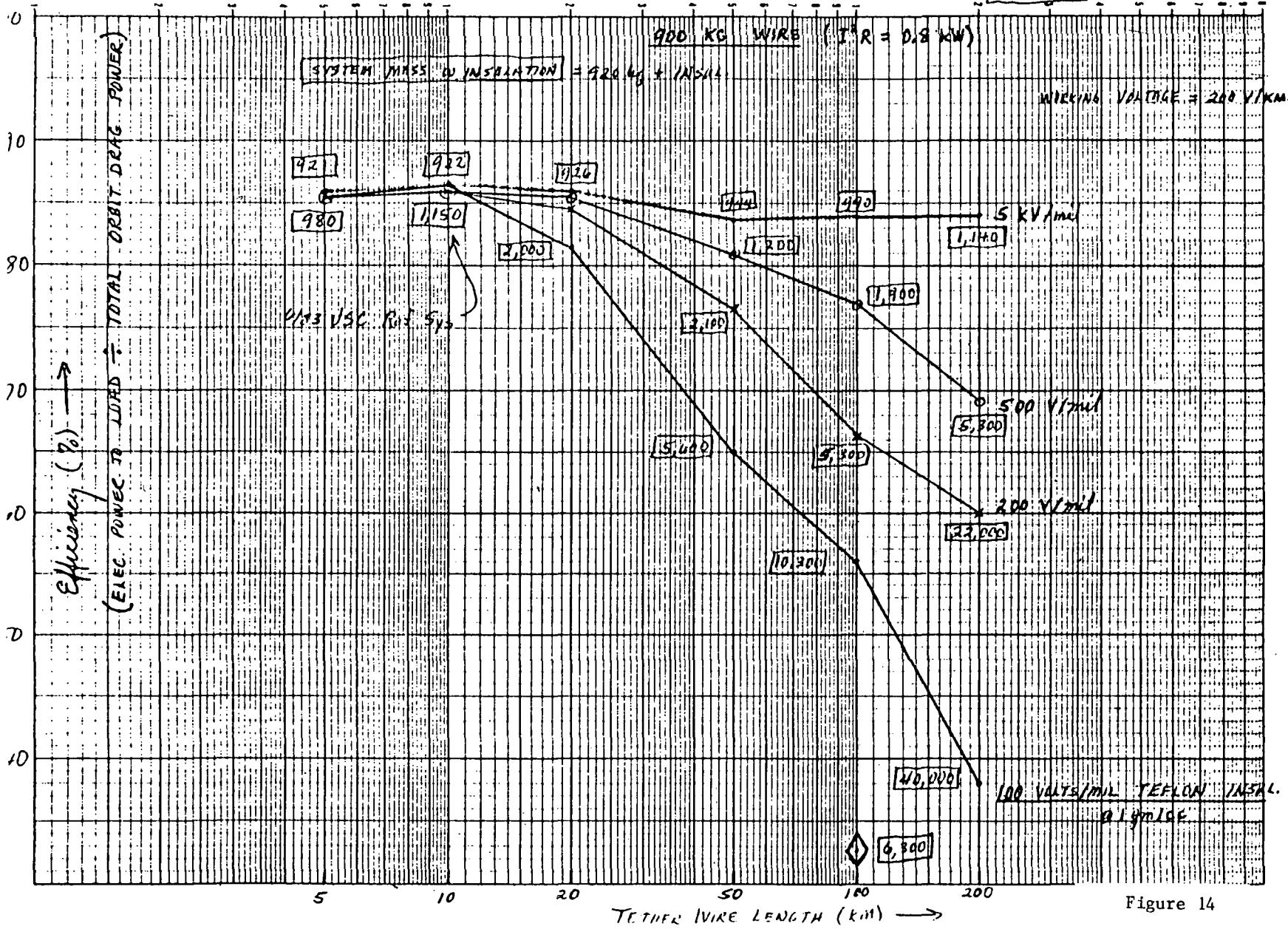


Figure 13

12/87  
McLoy

20KW PMG - EFF. vs WIRE LENGTH @ 260km ( $10^{-10}$  kg/m<sup>2</sup>)



ORIGINAL PAGE IS  
OF POOR QUALITY

Figure 14

Fig 1 - Tether Sever Rate (components)  
 From Meteoroids and Debris  
 (Aluminum Single Strand Tether)

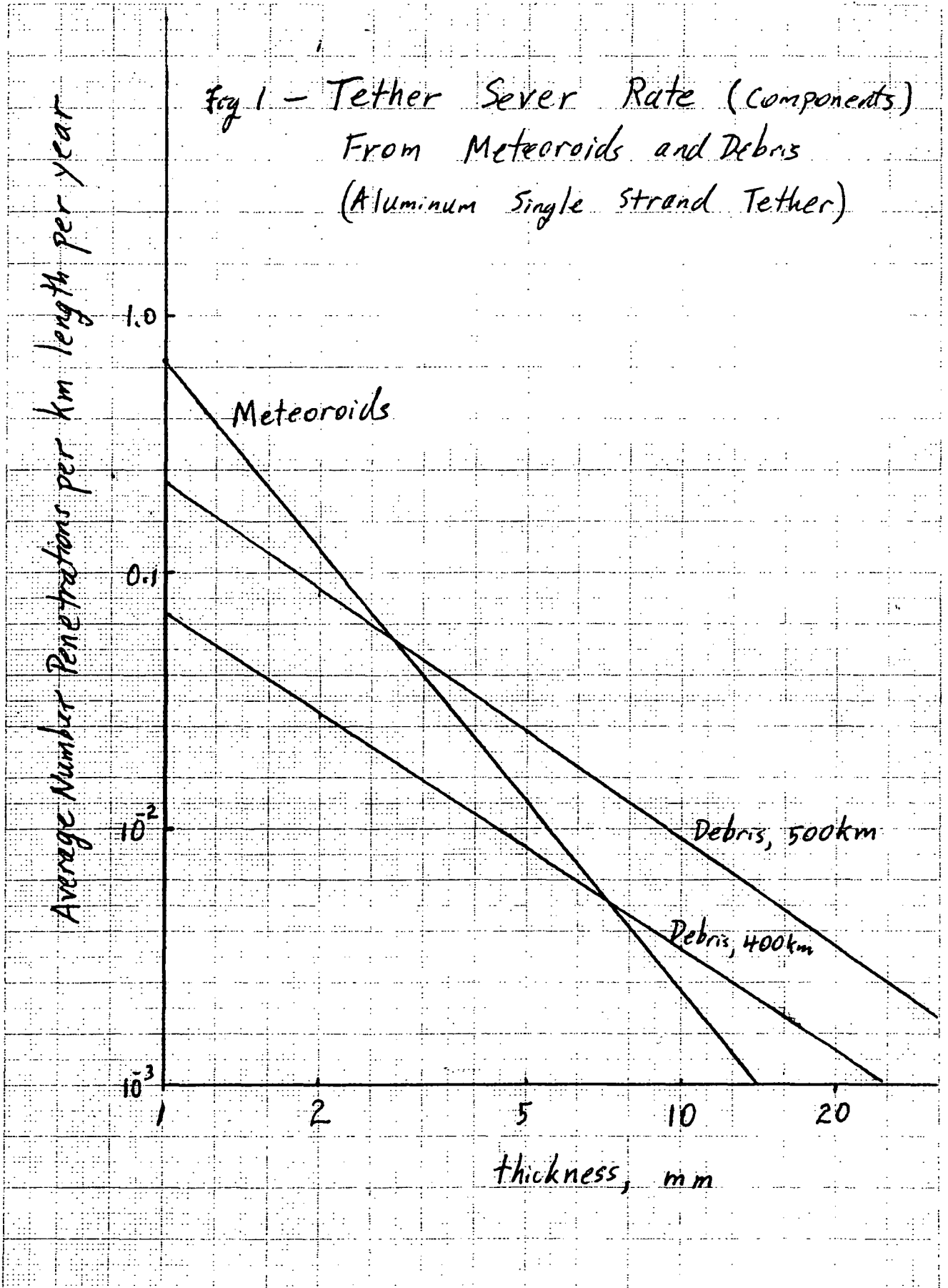




Fig. 2- Tether Sever Rate (Total)  
From Meteoroids and Debris  
(Aluminum Single Strand Tether)

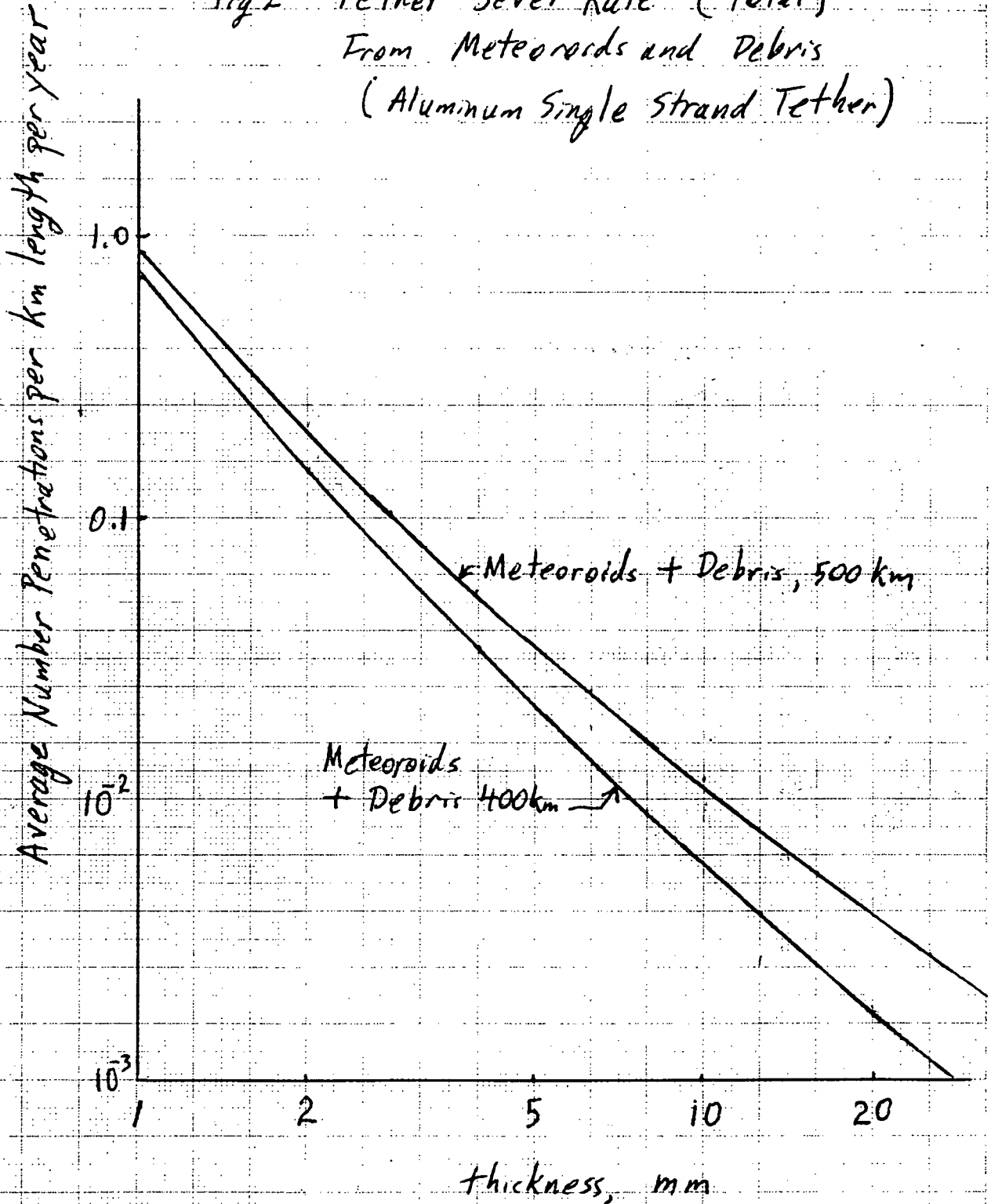


Figure 16

## MASSIVE TETHER DYNAMICS

TETHER WIRE MASS: 10-10,000 KG/KM

"SATELLITE" MASS: 10 KG → 0

STRAIN ELONGATION MINOR EFFECT

WAVE PROPAGATION ALL MODES

SHEAR

COMPRESSION

TORSION

"STRING"

3-D OUT-OF-PLANE MAGNETIC & CROSS-COUPLE TERMS

---

RUNNING CONDITIONS

ASSUME LOAD CONTROL REGULATION OF CURRENT (I)  
CONSTANT  $I \cdot V \longleftrightarrow IXB \cdot L$  WITH VARIABLE B,  $VXB$

ALLOW ARBITRARY STEP CHANGES IN  $I \cdot V$

REFLECT "USER" LOAD DEMANDS

DAY/NIGHT CYCLE REVERSALS OF POWER/THRUST

DYNAMIC CONTROL BY  $IXB$  PHASING ("CONTROL LAW")

ORBIT MANUEVER & CHANGE BY PHASED  $IXB$  THRUST

POWER STORAGE/PROCESSING by  $I \cdot V = d/dt(\text{ORBIT})$

APPLICATION

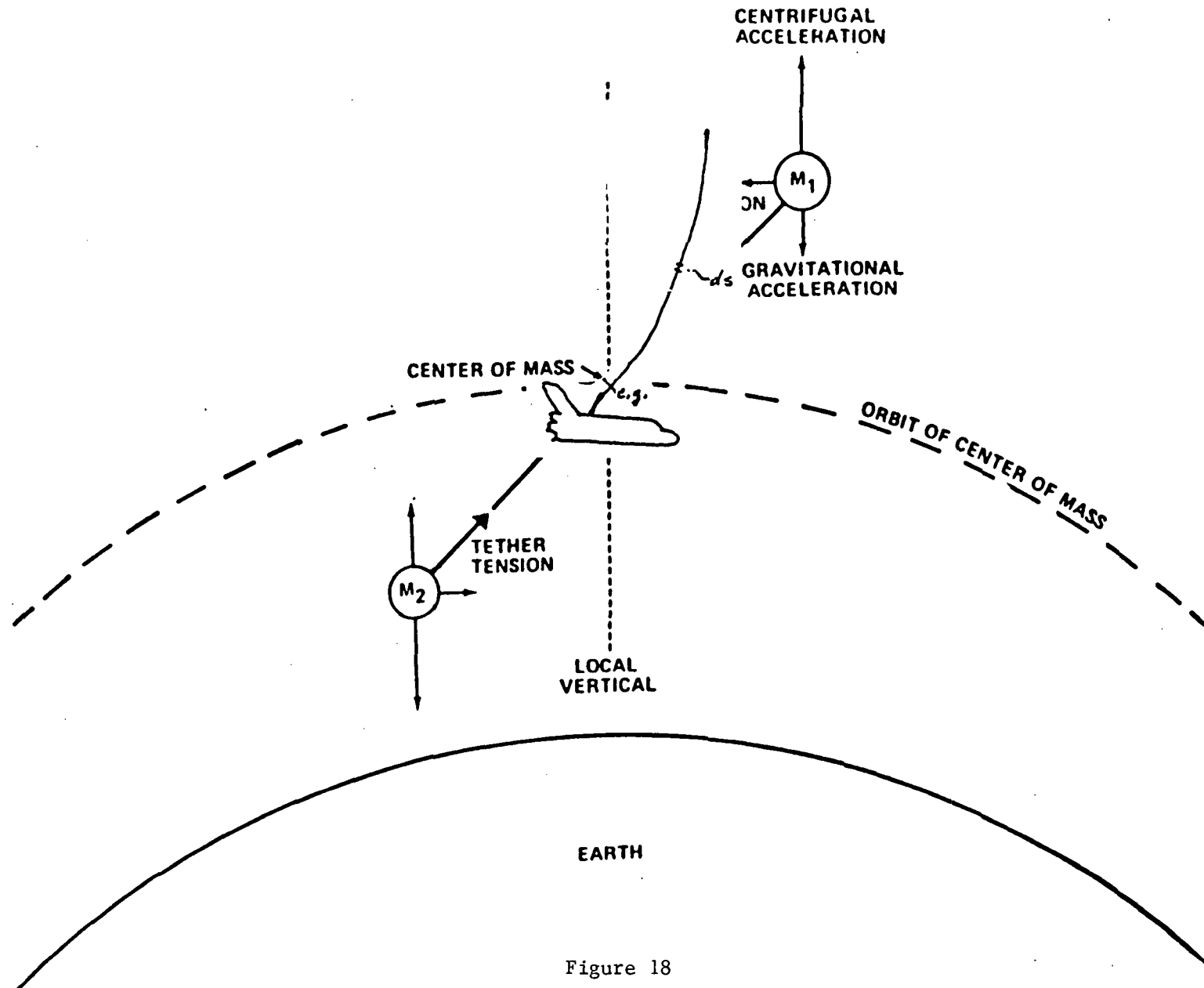
STABILITY LIMITS - IMPORTANT FOR 5-20 KM TETHERS

$IXB$  THRUST INTEGRATION/TRANSFER TO SPACECRAFT

MISSION PLANNING SIMULATIONS

MISSION "REAL-TIME" OPERATION PLANNING/PROJECTIONS

# FORCES IN TETHERED ORBITAL SYSTEM

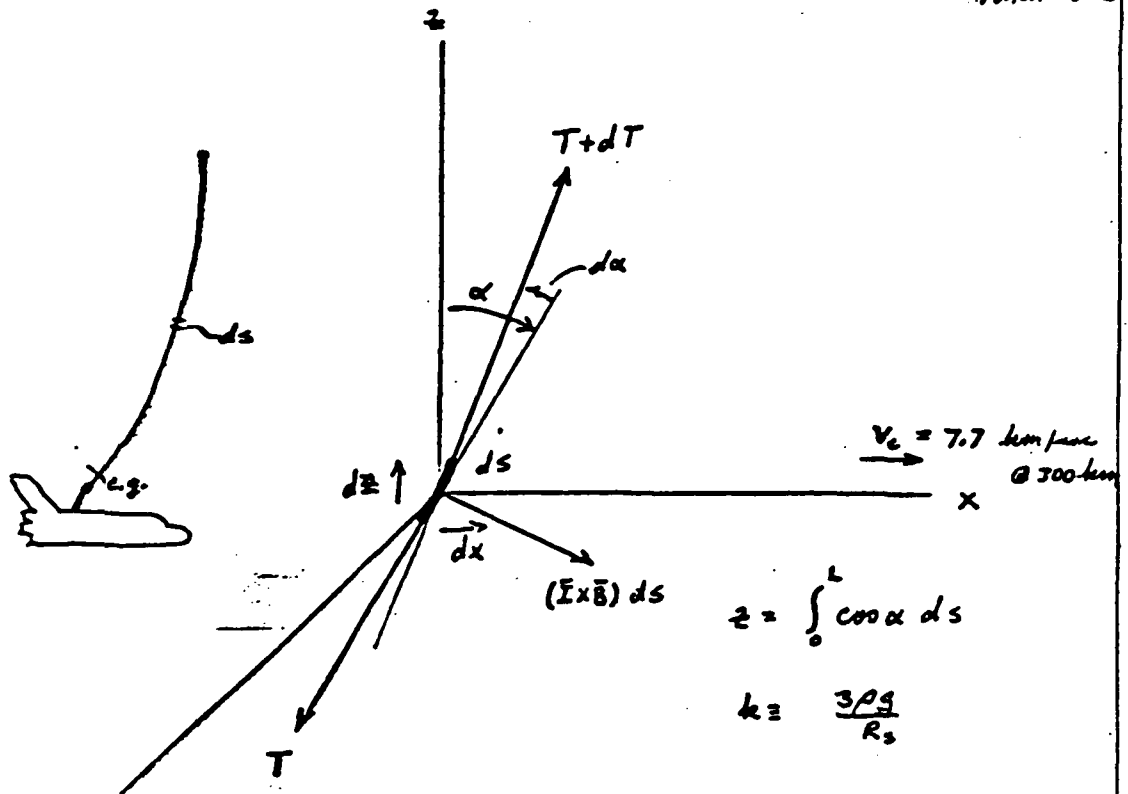


581

Figure 18

ELECTRO DYNAMIC TETHER

4/3/83  
J. P. C. C.  
NASA-JSC



- (1)  $kz \sin \alpha = IB + T \frac{d\alpha}{ds} \quad (+ \sum_i F_{xi} \cos \alpha)$
- (2)  $kz \cos \alpha = dT/ds \quad (+ \sum_i F_{yi} \sin \alpha)$

$$T(z) = T_0 + \frac{1}{2} k (z_L^2 - z^2)$$

$$\sin \alpha = \frac{IB - T (d\alpha/ds)}{kz}$$

$$(C_1 - \frac{1}{2} k z^2) X_{zz} + k z X_z - IB = \rho X_{tt}$$

$$\frac{\partial}{\partial z} \left[ (1 - \zeta^2) \frac{d\zeta}{dz} \right] + \frac{IB}{\rho} = \zeta_{tt}$$

Figure 19

$$u(z, t) = g(t) \eta(z) + W(z)$$

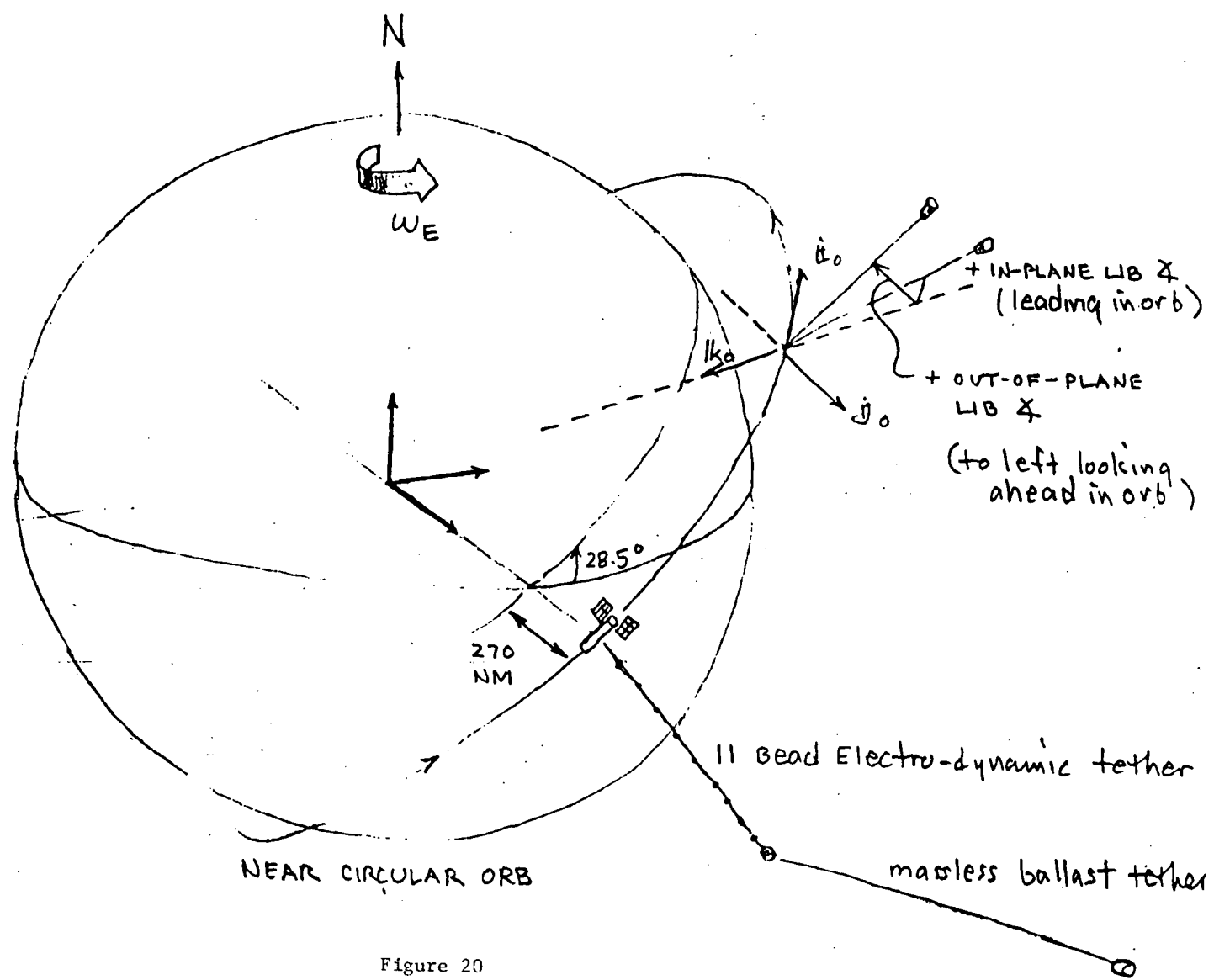
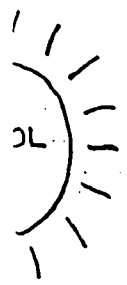
$$W(z) = \frac{2IB}{3\rho\omega^2} \ln(1 + \zeta)$$

$$\zeta = \frac{z}{L}$$

$$\nu_n = \omega \sqrt{(\frac{3}{2}) n(n+1)}$$

$$g(t) = A_n \cos(\nu_n t) + B_n \sin(\nu_n t)$$

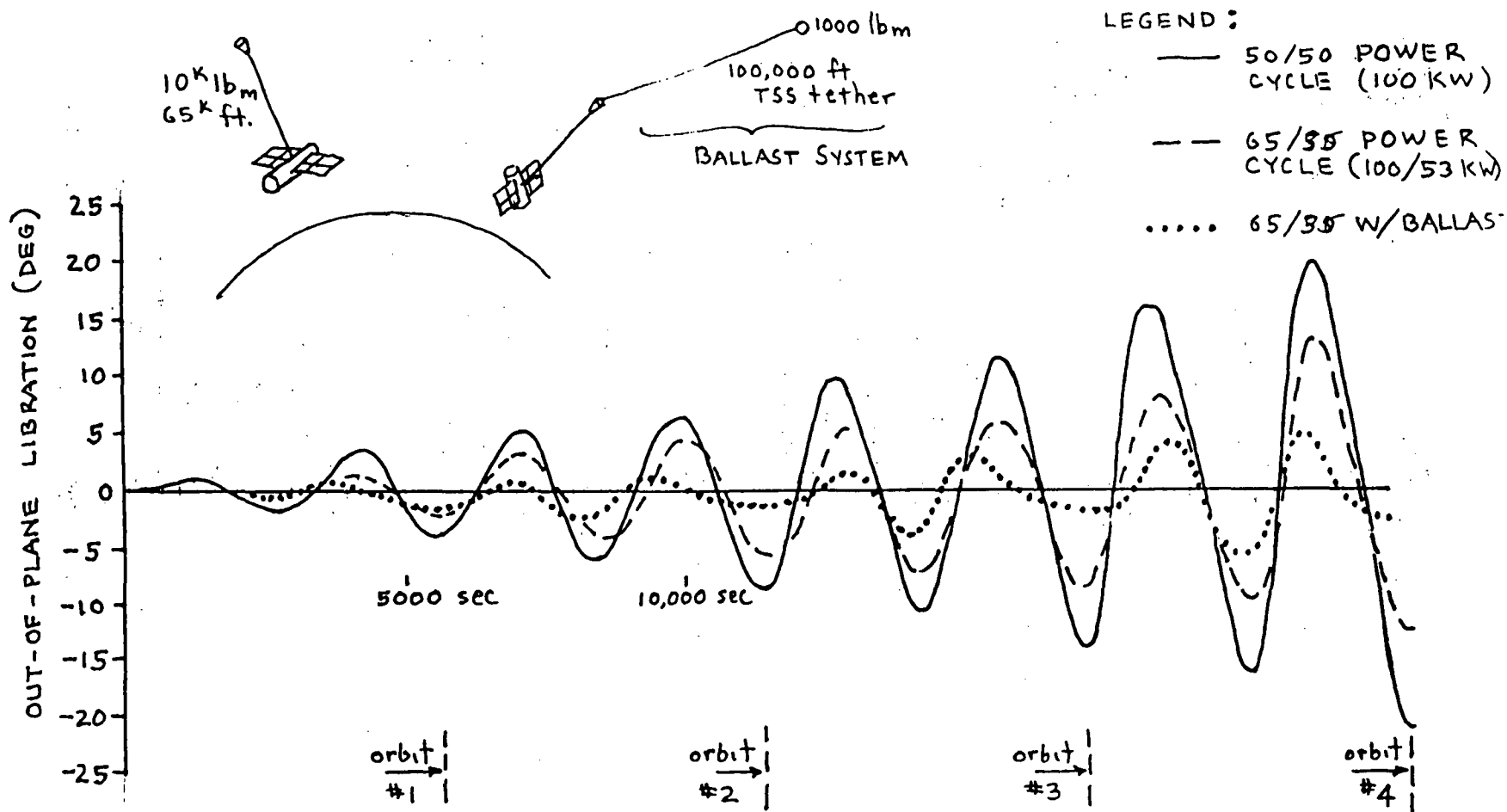
$$\eta(z) = P_n(\zeta) \quad n = \text{odd}$$



ORIGINAL PAGE IS  
OF POOR QUALITY

Figure 20

# OUT-OF-PLANE LIBRATION OF CONDUCTING END



584

Figure 21

# IN-PLANE LIBRATION OF CONDUCTING END

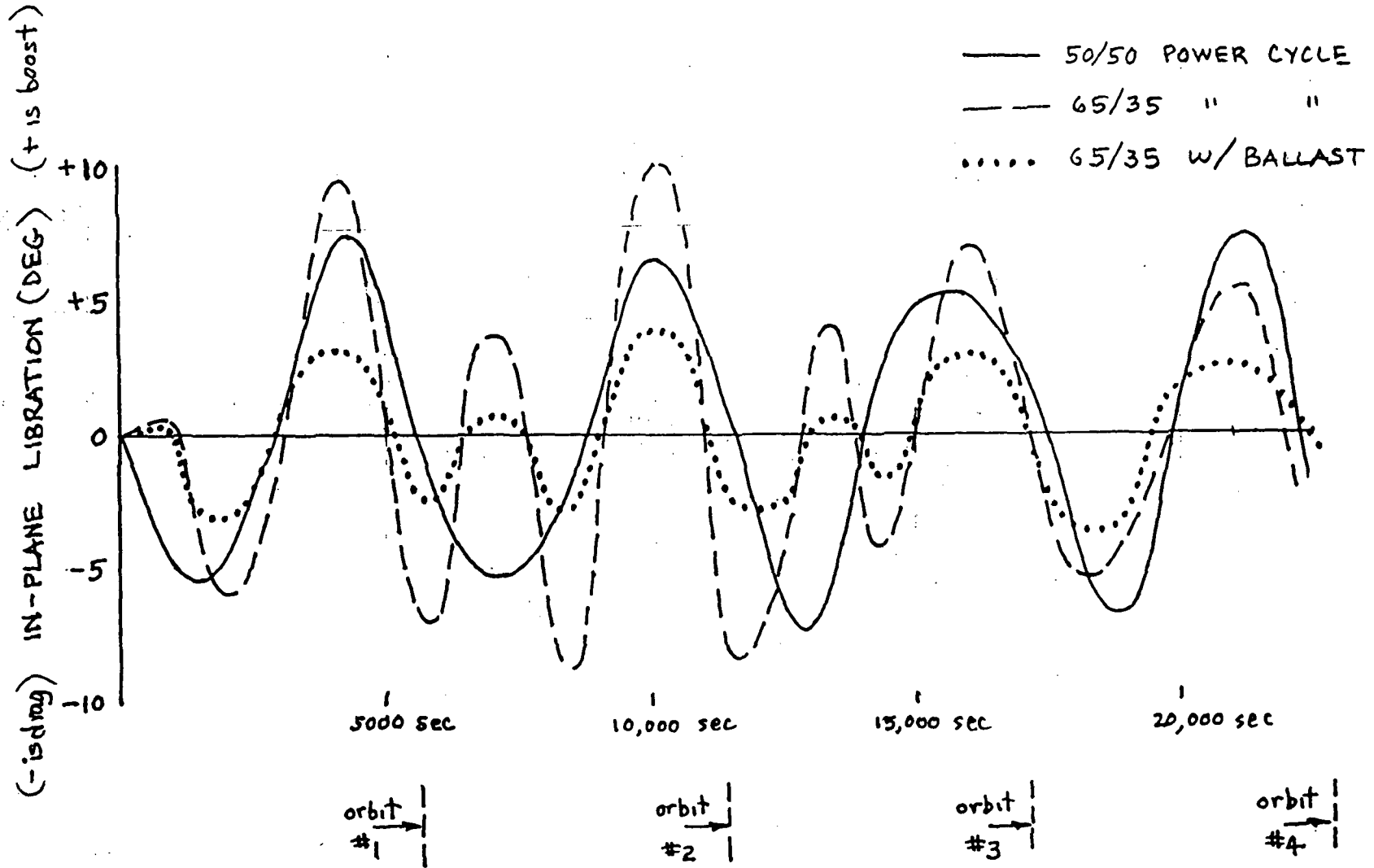


Figure 22

IN-PLANE LIB.  $\phi$  (DEG)  
(+ is leading)

5  
4  
3  
2  
1  
0  
-1  
-2  
-3  
-4  
-5

5000 sec

10,000 sec

orbit  
#1

orbit  
#2

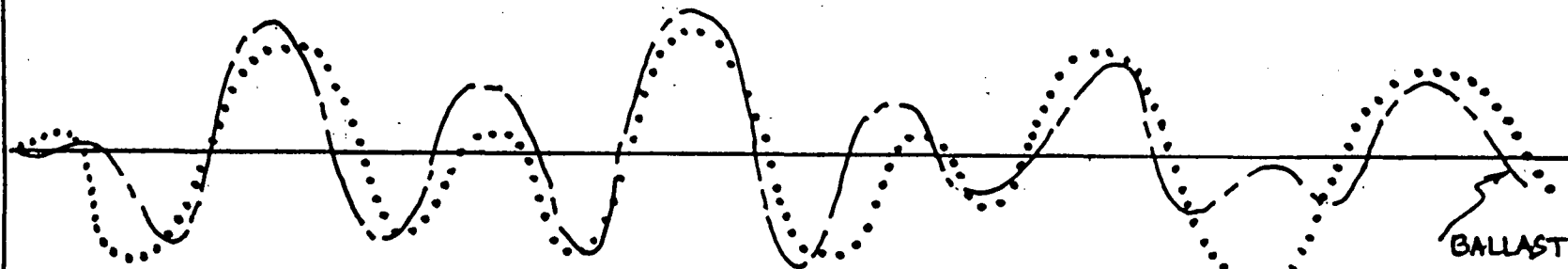
orbit  
#3

orbit  
#4

CONDUCTING END  
IN-PLANE LIBRATION

BALLAST MASS  
IN-PLANE LIB.

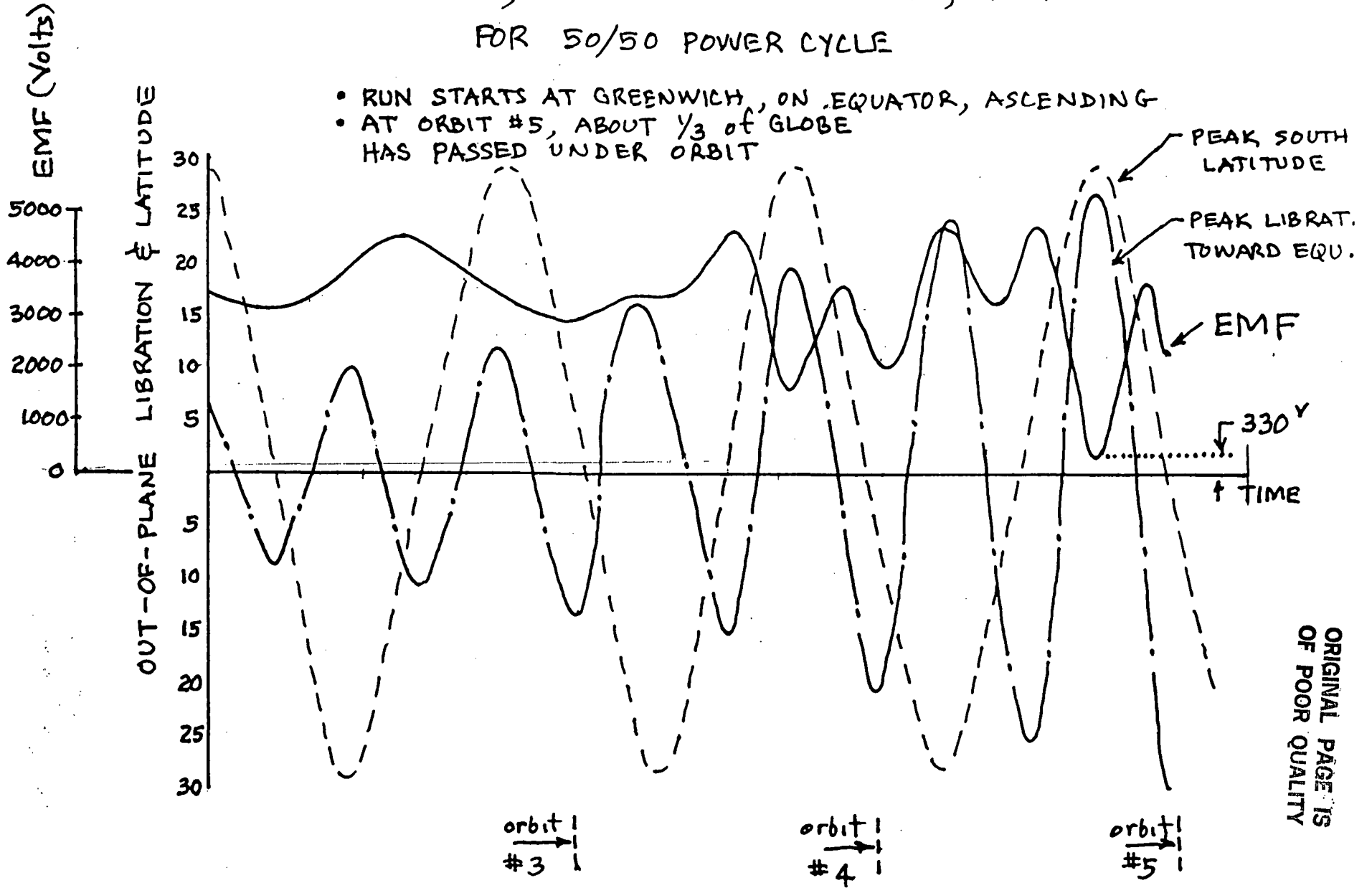
Figure 23





# LATITUDE, OUT-OF-PLANE LIBRATION, EMF FOR 50/50 POWER CYCLE

- RUN STARTS AT GREENWICH, ON EQUATOR, ASCENDING
- AT ORBIT #5, ABOUT  $\frac{1}{3}$  OF GLOBE HAS PASSED UNDER ORBIT



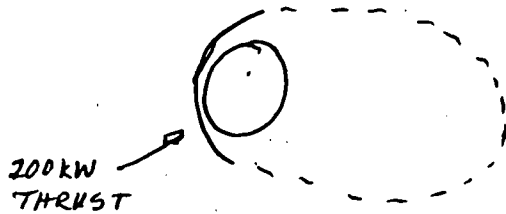
ORIGINAL PAGE IS  
OF POOR QUALITY

Figure 24

# PMG TETHER WITH "BALLAST"

APPLICATION: HIGHLY UNSTABLE POWER CYCLES WHERE IXB PHASING INADEQUATE

- 1)  $\frac{1}{2}$  ORBIT PERIOD OUT-OF-PLANE THRUST RESONANCE (PREVIOUS EXAMPLE)
- 2) LEO/GEO TRANSFER ORBIT "PUMPING"



2000 kg DTV : 6 DAYS @ 200kW

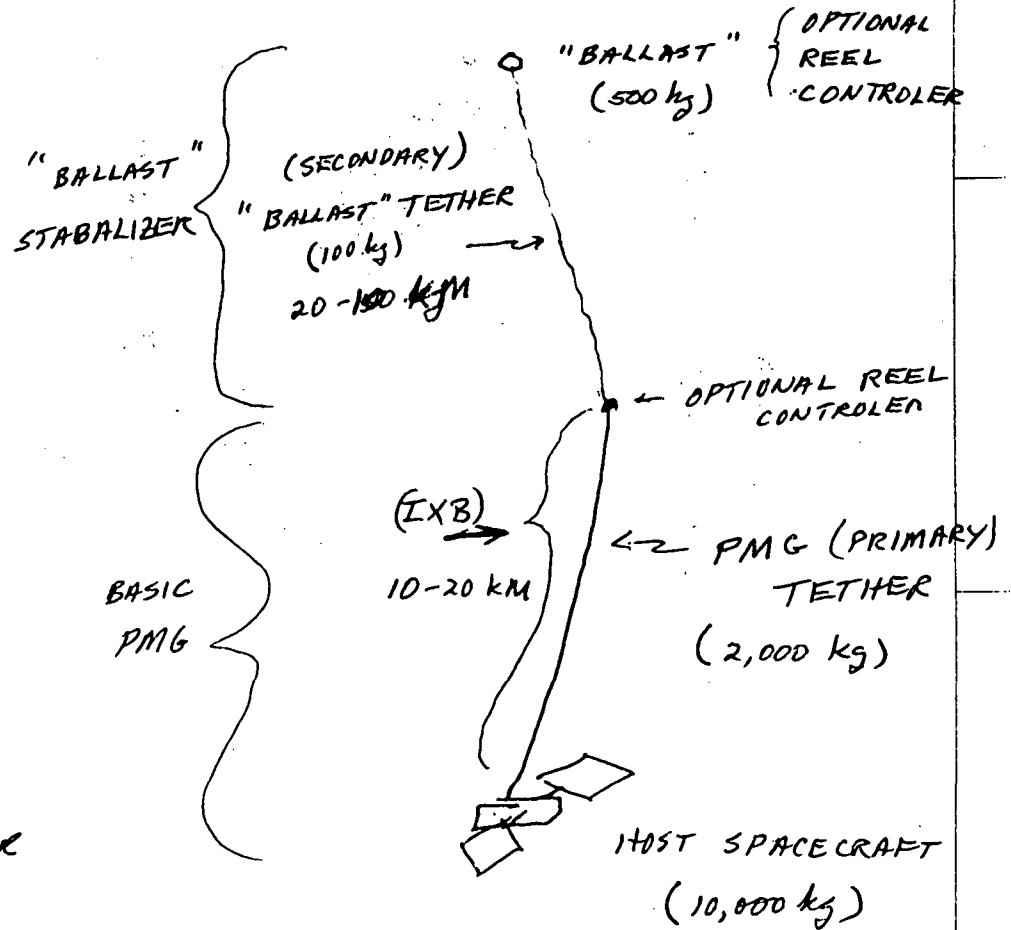
PROBLEM: ANGULAR RATE IN XFER CONTINUOUSLY VARYING. ( $\omega_0$ )

MUST KEEP TETHER ( $\omega_T$ ) IN PHASE

SOLN - RAPID VARIATION IN ANGULAR MOMENT. OF TETHER BY

USING "BALLAST" SECONDARY TETHER

AT END OF PMG TETHER



588

Figure 25

# JUPITER ORBIT ENERGY vs RADIUS

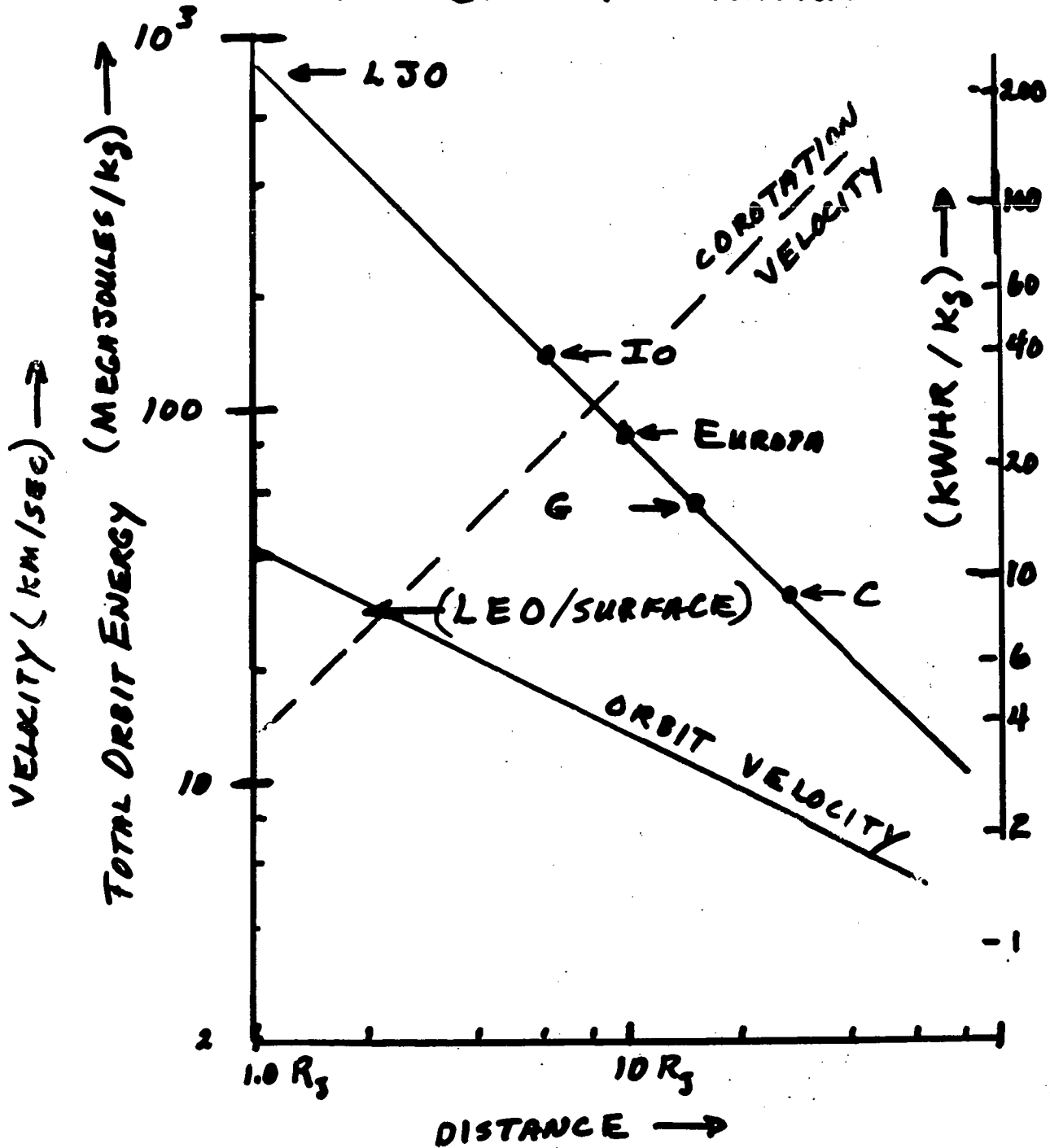


Figure 26

# TETHER VOLTAGE vs ORBIT RADIUS

$[V = V_A \sin \theta]$

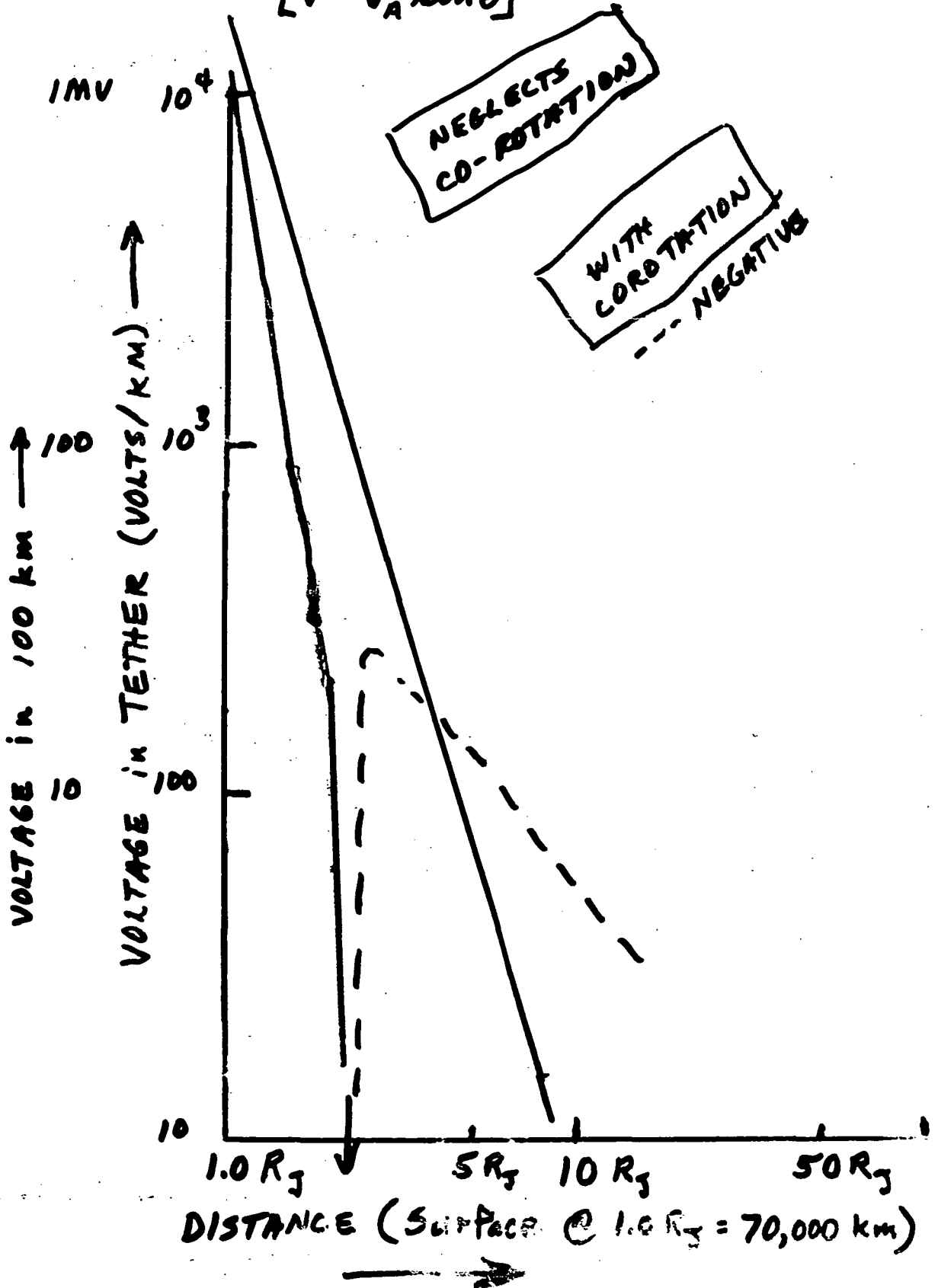


Figure 27

# JUPITER ORBIT

TETHER TENSION vs DISTANCE (CIRCULAR)  $\nabla G$

&

THRUST/DRAG FORCE vs ORBIT DISTANCE

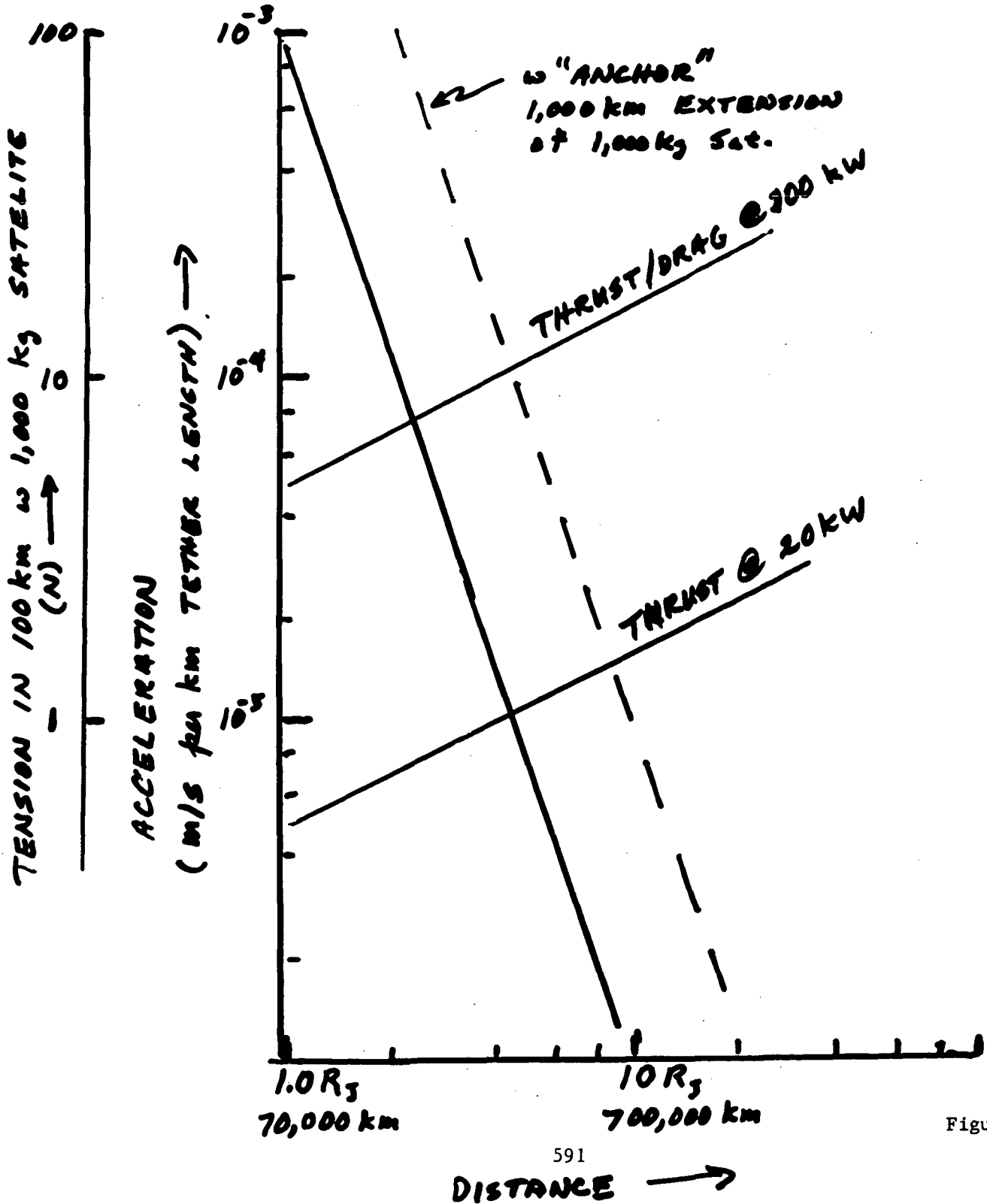


Figure 28



ORIGINAL PAGE IS  
OF POOR QUALITY

DATA TAKEN 9/25/85

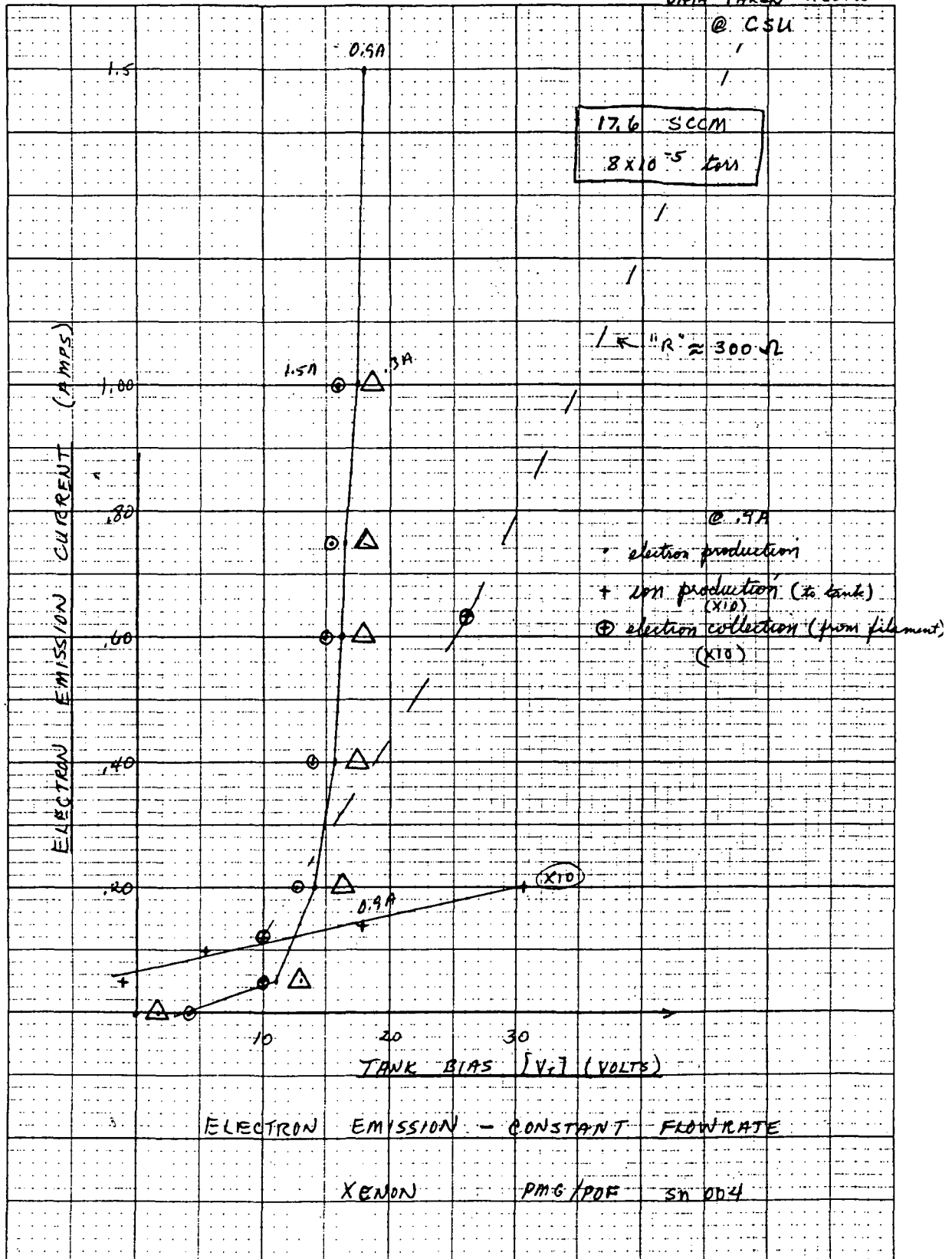


Figure 30

DATA TAKEN 8/26/85

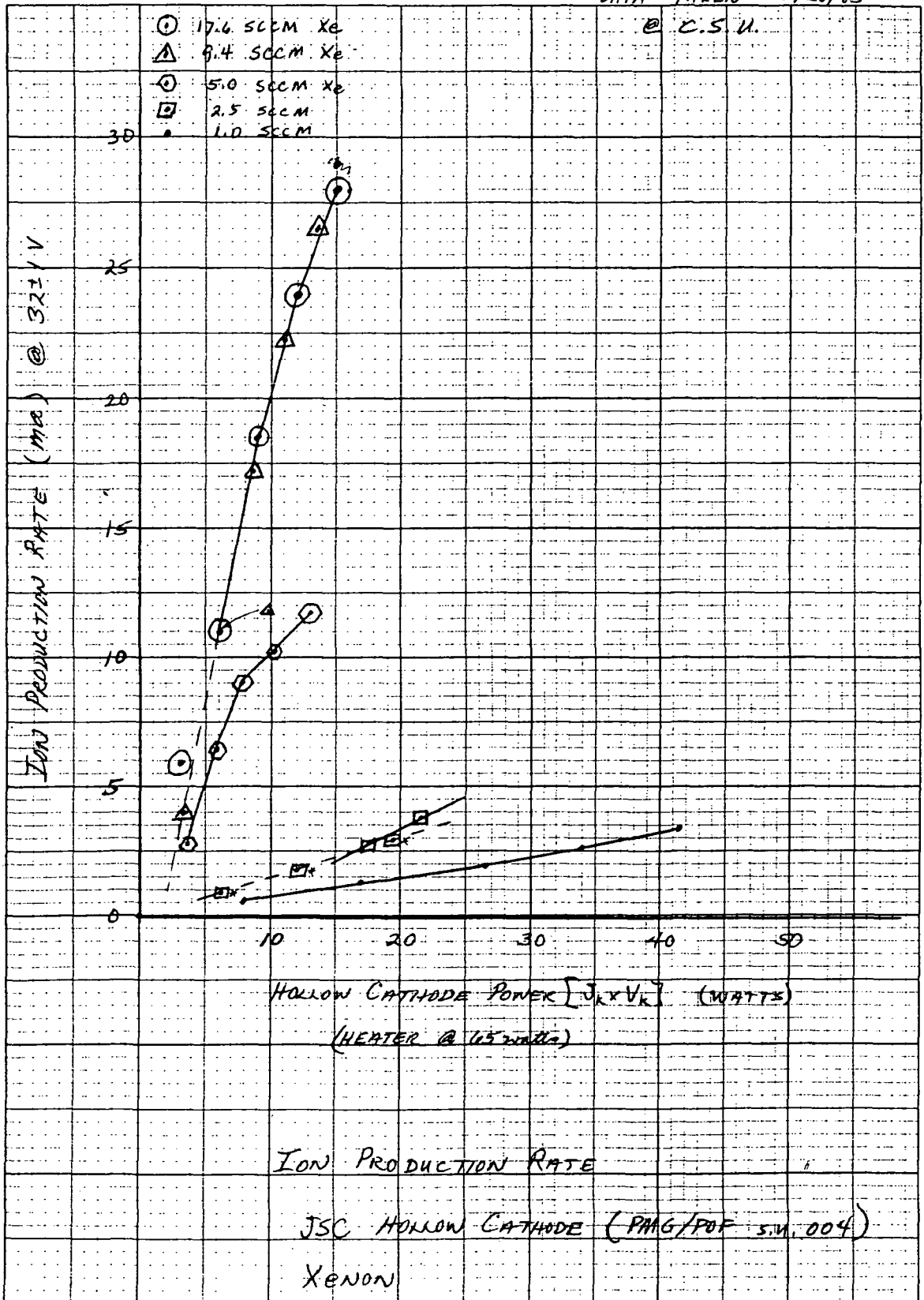


Figure 31